BIOPOLYMER MATRIX ENHANCES BONE REGENERATION IN RAT CRITICAL SIZE SKULL DEFECTS

Christina Karamini, B.D.S.

A thesis submitted to the faculty of the University of North Carolina at Chapel Hill in partial fulfillment of the requirements for the degree of Master of Science in the Department of Prosthodontics (School of Dentistry).

Chapel Hill
2006

Approved by

Advisor: Lyndon Cooper, DDS, Ph.D.

Reader: Ricardo Padilla, DDS, MS.

Reader: Nadine Brodala, DDS, MS, Dr med dent.

Reader: Glenn Minsley, DDS, MS.

Reader: Dina Dedi, DDS, MS.

ABSTRACT

CHRISTINA KARAMINI: Biopolymer matrix enhances bone regeneration in rat critical size skull defects.

(Under the direction of Dr. Lyndon F Cooper)

Reducing the need for harvesting autologous bone is a major goal of current research. A recently developed collagen/dextran hygrogel scaffold (E-matrix^{TM}) may offer osteoinductive advantages as a biologic polymer for bone repair. This scaffold, by mimicking embryonic extracellular matrix, could promote osteogenesis in the absence of osseoinductive agents. 8.9mm craniotomy defects were created in the parietal bone of 23 Sprague-Dawley rats. In a randomized manner, implants (Collagen only, Collagen/E matrix, Collagen/BMP) were placed onto the defect. Healing was permitted for 2, 4 or 6 weeks. At these timelines BMP treated defects showed good bone repair (26.20%, 42.60% and 22.12% bone fill, respectively). Ematrix^{TM} defects showed equal bone repair at 4 and 6 weeks (40.21 and 22.12% respectively), but reduced bone at 2 weeks (5.08%). Bone repair was incomplete in Collage and saline treated defects. Ematrix^{TM} supported bone repair of critical sized defects. The mechanism of action requires additional investigation.

ACKNOWLEDGMENTS

This three year endeavor would have been impossible without the help and support of many people that became involved in my research either from the beginning or sometime along the way. In either case their input was valuable in a unique way.

Foremost I wish to express my gratitude to my research mentor, Dr. Lyndon Cooper, for bestowing upon me the project along with the trust and hope that I would carry it through the way he envisioned it.

Dr. Ricardo Padilla whose constant care, support and unending help made the project actually work in every single step, I cannot say enough to thank him.

Mr. Ron Hill from *Encelle* for responding to our demands in materials for our project so promptly.

Dr. Nadine Brodala, whose recent experience in overcoming the hurdles and demands of a Master's thesis gave a lot of insight, help and support.

Drs. Glenn Minsley and Konstantina Dedi for their support and mentoring.

Dr. Daniel Caplan, for offering his input and establishing statistical validity in our results in the clearest way only he knows how to do, thank you.

Mr. Ian McCollum, thank you for making our histological findings as pretty as they could ever be!

Ms Donna Barnes and Karen Parker for kindly allowing Dr. Padilla and I to use their lab resources in order for us to carry out some histological analyses, earned their place in this list.

Dr. Steven Press for, so promptly, providing us with all the necessary material for our surgeries and making sure the experiments were run as smoothly as possible when I had more questions than answers.

Dr. Wagner Duarte and Dr. Harriet Arrington for immersing me in considerable, yet, most relevant literature.

Dr. Nimet Adatia for her support and help during the final stages of the preparation of this manuscript.

As I wouldn’t be able to be here, still I hope in sound mind, a big thank you to my parents and family for their unending support when it really counted and when it was mostly needed.

TABLE OF CONTENTS

LIST OF TABLES

LIST OF FIGURES

LIST OF ABBREVIATIONS AND SYMBOLS

MSCs	Mesenchymal Stem Cells
CSD	Critical Size Defect
ECM	Extracellular matrix
rhBMP-2	recombinant human Bone Morphogenetic Protein 2
BMPs	Bone morphogenetic Proteins
ACS	Absorbable Collagen Sponge
PPF	poly(propylene fumarate)
PLGA	poly(DL-lactic-co-glycolic acid)
PLA	poly(lactic acid)
PGA	poly(glycolic acid)
MMA	Methyl-methacrylate
PDGF	Platelet-derived Growth Factor
TGF	Tranforming Growth Factor
IGF	Insulin-Like Growth Factor
VEGF	Vascular Endothelial Growth Factor
MGV	Mean Grey Value
hr	hour
d	day
%	percentage

INTRODUCTION

The field of bone regeneration is rapidly evolving, and the use of osteogenic substances delivered to the wound site by means of constructs is one of the most promising methods to expedite new bone formation. The construct delivered to the site is impregnated preoperatively with a substance to enhance cellular and matrix functions and interactions, and have biocompatible and biomimetic properties close to the natural tissues. Our study will evaluate a new biopolymer as the matrix for the implanted constructs.

The use of vertebrate animal models for evaluating the healing of bone defects and for the testing of materials and methods for improving the repair of bone is a logical, established, and accepted procedure that closely resembles human clinical settings. We have selected the rat calvaria model for our experiments. The reason behind it lies on the fact that blood supply is only present at the base of skull at the area of muscle attachment into the skull. The critical size defect in the calvarium is a particularly good model (Sikavitsas et al. 2003) since it provides an excellent challenge to the tested material due to the lack of a primary nutrient artery, and its relative low marrow content. For these reasons the skull defect is considered the most severe bone implant test (Sikavitsas et al. 2003). The earliest scientific mention of a critical size skull defect was in 1889 by N. Senn who evaluated the healing process of trephined bone in dogs after implanting them with antiseptic decalcified bovine bone. Subsequently, the concept of "critical size defect" as currently understood has been defined by Schmitz and Hollinger (1986) as: *"the smallest size intraosseous wound that will not heal spontaneously during the lifetime of the animal."* This definition should be applied only to those defects created in adult animals, and healing is understood as development of new

bone. In the rat model, the defect should be a 0.8cm in diameter perforation through the calvarium (Sirola, 1960). Using this site is advantageous since no stabilization of the scaffold is required because the cranial site does not bear significant mechanical loads (Gysin et al. 2002).

Based on a recent literature review (Lutolf et al. 2003, Sikavitsas et al. 2005, Gysin et al. 2002), the rat model is a commonly employed model. We will utilize this model and try to follow standardized procedures in order to minimize the number and risk to the animal subjects, and to be able to compare our results with those obtained in the past by other institutions. In addition the significance of hBMP-2 will be tested in promoting osteogenesis as stated in studies by Reddi (1998).

Specific aim

As a first step in defining the role of this novel biomimetic scaffold (E-matrix), the osteoinductive efficacy will be tested using the rat calvaria critical size defect model. E-matrix will be delivered to 8.9 mm diameter calvaria defects in a collagen scaffold (Duragen®) and bone repair will be measured by histomorphometry after 2, 4 and 6 weeks of healing. hBMP-2/ collagen gel and empty defects will serve as positive and negative controls, respectively.

Clinical Significance

In the future, bone regeneration can be applied clinically where lack in bone mass can compromise or prohibit optimum treatment or when prognosis of final treatment is enhanced. Thus functional replacements for damaged or pathologic tissues can be made (Alsberg & Mooney, 2001) for example in recreating missing osseous structures (vertical bone loss), correcting craniofacial deformities and enhancing bone/tooth or bone/implant functionality and long-term stability (Earthman et al. 2003).

Bone regeneration and repair is of growing importance in dentistry. Reducing the need for harvesting autologous bone through the development of new biomaterials containing both osteoconductive and osteoinductive properties is a major goal of current research. Different approaches are now available and the majority of materials require the use of a scaffold or space filling material to direct bone formation in the targeted defect or extraskeleletal location. The various materials used as a scaffold for bone repair include autogenous bone, allogenic and xenogenic bone, and synthetic biomaterials. Recent investigations using synthetic resorbable polymers suggest an advantage of rapid biomaterial resorption, however, most of these synthetic polymers are not osteoconductive, osteoinductive nor osteogenic. Biologic polymers, (e.g. collagens) are often used as scaffolds for BMP-mediated bone repair. Other biologic polymer formulations may offer advantages of cell adhesion and stimulation for osteocondutive or osteoinductive bone repair.

A recently developed collagen / dextran hygrogel may offer osteoinductive advantages as a biologic polymer scaffold for bone repair (E-matrix^{TM}). This matrix may serve as a biomimetic of the immature / embryonic extracellular matrix and, as such, offer insoluble signals to mesenchymal stem cells for tissue repair / regeneration. Preliminary studies in this laboratory suggest this hygrogel is able to support bone repair. The goal of this project was to define the osteogenic potential of E-matrix for repair of bone using temporal evaluation of bone healing in the rat calvaria critical size defect model.

HYPOTHESIS

If osseous wound healing is controlled by mesenchymal cell / scaffold interactions, then a collagen/ proteoglycan scaffold capable of mimicking embryonic extracellular matrix will promote osteogenesis in the absence of osseoinductive agents.

LITERATURE REVIEW

TISSUE ENGINEERING

This project relies on the principle of tissue engineering, which according to Pollok & Vacanti (1996) is *the application of the principles and methods of engineering and the life sciences to the fundamental understanding of structure/function relationships in normal and pathological tissues and the development of biological substitutes to restore, maintain or improve function*. Tissue engineering provides the capability of creating specific, man-made tissues known as *neo-organs* that can overcome the problems associated with tissue transplantation (Langer & Vacanti, 1993). Tissue engineering approaches combine three main factors: reparative cells, signaling molecules and scaffold carriers (Reddi, 2000). In our project we tested a novel material (E-matrix^{TM}), a porcine collagenous matrix and its ability to induce endogenous and exogenous osteogenesis.

Osseous wound healing involves the recruitment of mesenchymal stem cells to perform the molecular tasks of bone regeneration. The initial matrix onto which these cells emerge is a key effector of bone formation or repair. Numerous materials are suggested as osteoconductive materials that support bone formation. A novel tissue-derived polymeric material has recently been used for cutaneous wound repair and is based on biomimicry of embryonic extracellular matrices. A collagen / proteoglycan scaffold (E-matrix^{TM}) has been used to promote healing of diabetic cutaneous ulcers. It is possible that this scaffold contains important molecular cues that enable stem cell function and support bone tissue repair.

Overall *a tissue-engineered implant designed to restore or modify the function of a tissue or organ is usually composed of a combination of biocompatible materials and biological components of the tissue* (Anderson, 1998).

Repair vs Regeneration

The repair of bone, as well as of any tissue, is a rapid process which has been selected through evolution to allow an animal to get up and move out of danger quickly. The wounded tissue is made avascular and thus becomes sealed off from the rest of the body (Davies JE, 2000, p.441). This ensures that micro-organism contamination does not spread throughout the body. The key to successful bone repair is the presence of high titers of mesenchymal stem cells (MCSs) that differentiate into a bridging cartilage mass in the avescular sector the connective tissue.

However, the regeneration of bone, is a much slower process than that of repair. In particular the regeneration at a cortical bone site of discontinuity, a thin monolayer of bone must form first at the inner or outer limit of the existing bone. This is followed by the formation of a layer of osteoblasts that produce thin sheets of osteoid which is densely mineralized. Vascular tissue always follows the layer of osteoblasts. The mineralization events always take place at a fixed distance from the secreting osteoblasts to ensure the separation of osteoid formation from mineral deposition.

Unfortunately, we are still uncertain of the key factors controlling the formation of the whets of osteoblasts and therefore unable to proceed with the design of tissue-engineered cortical bone that follows the regeneration pathway. Thus, we must focus on the repair pathway for the purposes of bone engineering.

Several key factors have been identified in the repair of bone (Davies JE, 2000, p.442):

1. Well-defined boundaries of the defect must be fully occupied by the implant material to inhibit dysfunctional fibrosis.
2. MSCs must migrate into or be placed within these boundaries.

3. These boundaries must be occupied by a cell-delivery vehicle that either is resorbed or becomes functionally integrated into the new structure.
4. Adequate vascular supply must be present and must aggressively communicate with the entire length and depth of the defect for the supply of nutrients and chemotactic/ osteogenic factors.
5. Lastly, osteogenic bioactive factors which target and affect MSCs and their lineage descendants as well as the vascular network must be present.

SCAFFOLDS/ DELIVERY VEHICLES

As mentioned above, the use of delivery vehicles is essential in the bone engineering process. Approximately over 500,000 bone grafts are performed in the United States to repair or regenerate diseased or missing bone. Although autologous bone grafts have been long established as the "gold standard" for such procedure they are fraught with a number of complications mainly including chronic pain and physiologic impairment of the donor site, infection, hemorrhage, nerve damage and cosmetic deformity. In addition the use of allograft materials, as an alternative material for bone reconstruction, has been problematic with regard to their immunogenicity, compromised biomechanical and physiological properties as well as potentially limited supply. Thus, researchers have been focusing into engineering synthetic, three-dimensional bone scaffolds made from polymeric materials onto which cells or growth factors can be incorporated to induce normal bone formation (Hollinger *et al.*, 2005, p.150).

These scaffolds should encompass the characteristics of biofunctional and multiphasic properties of delivery vehicles. Such scaffolds should house or attract progenitor cells capable of progressing down the entire chondrogenic lineage to the end-stage phenotype, calcified hypertrophic cartilage. In other words, they must organize, in a defined volume with

precise boundaries, the differentiation of cartilage that can be rapidly replaced by endochondral bone. This is the first phase in the multiphasic process of bone repair. Secondly, the ideal vehicle should exhibit bioactivity unique to the first phase and preferably dissolve to initiate and contribute to the second phase. (Davies JE, 2000, p.457)

Biodegradable scaffolds offer the possibility of replacing osseous tissue and overcoming problems such as infection and device dislocation which are associated with permanent implants (Davies JE, 2000, p.454)

Further to these inherent biological properties, scaffolds need to fulfill the following physical properties based on the mechanical loading demands of the defect site:

1. The scaffold should be easy to handle in the preparation and implementation of the implant materials
2. It should be highly porous to allow rapid vascular ingrowth into the defect area.
3. It should maintain the space for differentiated and specialized extracellular matrices and structural components. The material should be strong enough to withstand physiological stresses, yet, a lack of sufficient mechanical stimulation may result in poor tissue regeneration and/or bone resorption around the implant. (Davies JE, 2000, p.455).
4. It should be easily adjustable/ moldable to fit the defect or surgical site.
5. It must exhibit a reproducible and controlled breakdown or dissolution process in every insertion site. Since the scaffold's mechanical strength usually decreases as it degrades, the degradation rate should be coupled to the rate of tissue regeneration in order to maintain the structural integrity of the construct (Davies JE, 2000, p.455)

Thus, such properties must not be affected by the host's response or the implantation site.

Further to the properties mentioned above, the delivery vehicle must be biocompatible and thus fail to evoke an extreme adverse inflammatory or immune response once implanted (Davies JE, 2000, p.456). An important point is that the scaffold's biocompatibility, as far as the material's chemical and physical structure and physical morphology is concerned, can be affected by synthesis or processing techniques.

Another important aspect in the manufacturing of scaffolds is the method of sterilization, which must not interfere with the bioactivity of the material, or significantly alter its chemical composition and consequently its biocompatibility or degradation properties (Davies JE, 2000, p.456).

Application of scaffolds

Tissue growth

Tissue growth involves cellular migration from the host tissue into the scaffold to form new tissue. In this case, the scaffold only acts as a substrate to encourage migration and proliferation of the desired cell types. It has been shown that both poly(propylene fumarate) (PPF) and poly(DL-lactic-co-glycolic acid (PLGA) are able to attract osteoblasts into the defect site (Davies JE, 2000, p.456).

Cell transplantation

In this application, the delivery vehicle should not only demonstrate migration of native cells into the defect but also support proliferation and differentiated function of seeded cells. For the purposes of bone regeneration, stromal osteoblasts and osteoblasts from the donor are seed onto the scaffold and expanded in culture prior to the transplantation of the construct to the patient. Both PPF and PLGA have been shown to support in vivo these functions (Davies JE, 2000, p.457)

Delivery of bioactive molecules

Examples of these molecules include bone morphogenetic proteins (BMPs), transforming growth factor beta-1 (TGF-β1) and hormones (e.g. oestrogen, thyroxin). Controlled delivery of these factors to aid in bone regeneration is often desired, eventually leading to the incorporation of the bioactive molecules into the implantable scaffolds. Loading procedures can either involve binding of the molecules to the polymer during the scaffold processing or loading onto bioresorbable nanoparticles that become entrapped within the scaffold. (Davies JE, 2000, p.457)

Prevascularisation

This application can be used to allow the ingrowth of vascular tissue (either fibrovascular or periosteal) before cell seeding. Such application is considered since the rate of vascularisation is often insufficient to prevent cell death within the implanted construct. Bone defects created after tumour removal particular benefit from prevascularisation because the recipient tissue bed is commonly undermined in its ability to support vascularisation due to abnormal local bone physiology and the necrotic effects of locally delivered radiotherapy (Davies JE, 2000, p.457). In this case, polymer scaffolds are implanted onto a periosteal site remote to the defect and allowed to form vascularised bone prior their re-implantation to the defect site (Davies JE, 2000, p.457).

Scaffold materials

Preformed

They are the most widely investigated types of scaffolds and have been associated with cell transplantation applications. These delivery vehicles are more biocompatible since residual

toxic chemical can be removed by leaching them in water after processing them. Cells can be seeded onto these scaffolds and cultures in vitro prior to the construct's implantation. In this way the production of large sections of tissue is possible prior to implantation. Examples of such scaffolds are PLA, PGA, PLGA, and PPF. Other less extensively tested polymers include pseudo-poly(amino acids), poly(carbonates), poly(acrylates), poly (phosphates), poly(phosphazenes) and poly(anhydrates) (Davies JE, Bone Engineering, p.458).

The most extensively used group of polymeric scaffolds belong to the family of poly(α-hydroxy acids) which include poly(lactic acid) (PLA) and poly(glycolic acid) (PGA) and their copolymers. PLA exist in two enantiomeric isomers of lactide (D and L). PLA degrades to lactic acid which is further metabolized yielding CO_2 and water. The copolymerization of the two enantiomeric forms yields PDLLA which is clinically applied in craniofacial fixations.

PGA is a highly insoluble polymer and its solvent, hexafluoroisopropanol is highly toxic. For this reason PGA is used as a copolymer with PLA. When degraded to glycolic acid it is metabolized in the body.

The copolymer of PLA and PGA is poly(lactic-co-glycolic acid) (PLGA) and it has been extensively studied in tissue engineering projects. The copolymer was initially introduced as "LactoSorb" manufactured by Lorenz Surgical Inc. It has been shown to completely resorb in 12 months (Hollinger *et al.*, 2005, p.152) and has been used in pediatric craniofacial reconstruction.

Injectable

Such polymers can more easily fill defects of various sizes and shapes, requiring minimal surgical intervention. Liquid and gel scaffolds which belong to this category function to physically entrap cells destined to be implanted in the defect site. However, such scaffolds lack in mechanical strength and therefore cannot be used in load-bearing defects such as those in orthopaedic cases. Nevertheless they are amenable to polymerization and cross-

linking in situ should additional strength be required. Alternatively it has been reported that PPF is often combined with ceramic particles such as β-TCP, calcium carbonate or calcium phosphate for use in orthopaedics (Davies JE, 2000, p.459). Another advantage of these scaffolds is the presence of large number of interconnected pores that promote bone ingrowth.

Curing of these scaffolds is initiated by chemical means or via the use of light. Cross linking agents include methyl-methacrylate (MMA). Also the degradation and mechanical properties of these materials can be achieved via photopolymerisation with particles or different linear polymers within them, resulting in interpenetrating polymer networks.

HYDROGELS

This type of scaffolds permit the retention of large amount of water on the polymer without causing it to dissolve. They share many characteristics with biological tissues, namely their permeability to small molecules and their low interfacial tension. Although hydrogels do not possess increased mechanical strength to support loaded skeletal structures, they provide a matrix for accelerated tissue formation which will in turn provide mechanical integrity. Alginate, pluronics, chitosan and fibrin glue are some examples of hydrogel scaffolds.

In addition to the aforementioned properties of scaffolds, hydrogels in particular should encompass the following characteristics according to Temenoff & Mikos (2000):

1. Biocompatibility and non-toxic degradation products
2. Sufficient mechanical strength for the intended applications
3. Ability to promote tissue formation
4. Sterilizability to prevent infection
5. Be able to polymerize on a clinically acceptable time scale with a minimal temperature change
6. Promote ease of handling by the surgeon

Cells can be encapsulated during hydrogel formation and the latter can be fabricated *in situ* within the defect site in the body. The porosity of these scaffolds can be modulated by altering the cross-linking density (Elisseeff *et al.*, 2005).

Chen *et al*., (2003) looked into the efficacy of an injectable form of hydrogel to induce bone tissue. They utilized a temperature-depended polymerizing polyethylene oxide hydrogel as a vehicle to deliver bone marrow mesenchymal cells in rats. After an observation period of 2 months they found that areas of mature endochondral bone exhibiting trabeculation and abundance of bone matrix and osteocytes enclosed in lacunae. Although this method eliminates the invasive procedure of conventional bone grafting it poses the inherent problem of confining the injectable bone and fine molding into the desired contours at the defect site.

In an *in vitro* study by Mikos' group (Payne *et al*., 2002) it was shown that bone marrow stromal cells exhibited much higher viability, proliferation and phenotypic expression when they were encapsulating in actively crosslinking PPF composites rather than their non-encapsulated counterparts in a test period of 28 days.

Alginate, a polysaccharide, is extracted from seaweed that forms an ionic gel in the presence of divalent cations such as calcium. It has been extensively studied *in vitro* and *in vivo* as a scaffold for cartilage replacement and engineering, in the craniofacial region.

To address tissue engineering of osteochondral tissue, a multilayered hydrogel system was developed (Elisseeff *et al*., 2005). This system allow for distinct cell types to be co-cultured in 3 dimensional systems.

Bosnakovski and co-workers (2006) showed the osteogenic and chondrogenic effect of type I collagen hydrogel in combination with TGF-β1. Yet, they found that collagen type II was the most favorable one for expressing chondrogenic phenotype as it resulted in the upregulation of chondrogenic genes and synthesis of type II collagen and GAG.

Trojani *et al*., (2006) in an *in vivo* study examined the osteogenic effect of self-hardening Si-hydroxypropylmethylcellulose (HPMC) in conjunction with HA/TCP when it was injected

subcutaneously (SC) and intramuscularly (IM). They found that after 8 weeks of implantation mineralized woven bone was present markedly invaded by numerous osteoblasts. Increased amount of active osteoclasts attached to the HA/TCP particles and small vessels being homogenously distributed in the entire area of the implant was also observed histologically. The lack of fibrous encapsulation of these particles proved good osseointegration of the composite into the surrounding tissues. Si-HPMC is a hydrogel with hardening time of 10 minutes which allows for manipulation in *in vitro* applications and injection in *in vivo* settings. The hydrophilic polymeric phase of the hydrogel makes the material injectable and when hardened it serves as a space-holder to prevent granule packing and providing for homogenous delivery of cells into the recipient site.
Overall this model provided evidence for a novel method of osteoinduction with promising result for possible future application.

Scaffold fabrication

The main goal in scaffold fabrication is to introduce porosity in a three dimensional network which is essential in bone regenerative procedures. Some of the most important techniques are summarized below.

Particulate-leaching

Porogen leaching was patented by Mikos and his co-workers in 1996 (Hollinger *et al.* 2005, p.159). In this technique water soluble particles (salt, sugars or polymer spheres) are dispersed in a matrix comprising of the scaffold material dissolved in an organic solvent. This process can yield the following:

1. "skin" of nonporous polymer at the surface
2. non-homogeneous dispersion of pores
3. lack of inner connectivity of the pores, and
4. remaining porogen within the scaffold after porogen leaching.

Emulsion Freeze-drying

In this technique a homogenized emulsion of the polymer solvent solution and water is created. The solvent and the water are then removed by freeze-drying after the mixture is rapidly quenched in liquid nitrogen. The advantages of this technique include the ability to control the pore sizes from 15 to 200 microns and the ability to obtain porosity in excess of 90%.

Phase separation

This technique involves the demixing of homogeneous polymer/ solvent solution into both polymer-rich and polymer-poor phases. Unlike freeze-drying method it does not involve the homogenization of the mixture. A modification procedure, termed as “coarsening effect”, was applied to the original technique of phase-separation to increase the pore size from 1-20 μm to greater than 100μm. A clear disadvantage is the use of dioxane as a solvent, which is a suspected carcinogen.

3D Printing

A complex 3-D structure is constructed by a polymer powder packed with salt particles. This structure is subjected to a solvent selectively applied. Subsequently the polymer/ salt composites are submerged into water to dissolve the salt particles resulting in porous devices with micropores (45-150μm). This is a relatively new method.

Gas foaming

CO_2 is used in this method to create porosity which allows for the application of growth factors onto the scaffold. Unfortunately in this technique the pores are not interconnected.

Polymer Microspheres and Growth Factor delivery

The properties and importance of the different growth factors in bone engineering will be reviewed in the upcoming chapter. In this section, however, emphasis is placed on how these important molecules can be locally delivered and administered to the grafted sites.
Adsorption of growth factors onto the polymer scaffolds' surface is one method of delivery (Hollinger *et al.*, 2005, p.160). Yet, this method does not allow for the precise and controlled release of the growth factor over time onto the target site. For this reason researchers looked into the encapsulation of growth factors within polymeric microspheres which are then incorporated within the scaffold.

Polymer microspheres are hollow capsules and are commonly fabricated from either synthetic or naturally occurring polymers, such as PLGA and gelatin respectively. Techniques for their fabrication include water/oil/water emulsion or oil/water emulsion or spray-drying. The encapsulated growth factors are released in a controlled manner over a period of time once the polymer begins to degrade.

Hu *et al.,* (2001) reported controlled release of a model protein (bovine serum albumin, BSA) after it became encapsulated within PLGA microsphere that had been coated with poly(vinyl alcohol). An additional study by Meese *et al.*, in 2002 (Hollinger *et al.*, 2005, p.161) confirmed the feasibility of this approach.
Ambrosio and co-workers in 2001 (Hollinger *et al.,* 2005, p.161) developed a novel technique involving sintering of PLGA microspheres to form a porous scaffold. However, this method precludes the incorporation of growth factors into these carriers due to the use of heat in this procedure.

In 2001 Richardson *et al*., (Hollinger *et al*., 2005, p.161) described the fabrication and evaluation of a poplymer scaffold that delivered two growth factors for bone regeneration in the context of therapeutic angiogenesis. In this study vascular endothelial growth factor (VEGF)-165 and platelet-derived growth factor (PDGF)-BB – growth factors with distinct kinetics – were incorporated into a single polymer scaffold. The project showed the rapid formation of a mature vascular network and the researchers emphasized not only the success of such a scaffold but also the necessity for delivery of multiple growth factors for significant clinical application compared to the limited application of single growth factor delivery.

SIGNALING MOLECULES

Growth Factors

They are hormones that are best characterised as activity modulators. They can either stimulate or inhibit cellular proliferation, differentiation, migration, adhesion, apoptosis and gene expression (Hollinger *et al*., 2005, p.126).

Insulin-like growth factors (IGFs), bone morphogenetic proteins (BMPs), fibroblast growth factors (FGFs) and vascular endothelial growth factors (VEGFs) are some of the secreted soluble growth factors that play an important role in wound healing by regulating chemoattraction, mitogenesis and differentiation (Hollinger *et al*., 2005, p.126). The spatial localization of growth factors drives the temporal sequence of wound healing. (Hollinger *et al*., 2005, p.126). Yet, one of the major obstacles for tissue engineering of bone is to control the spatial gradients of wound healing factors.

Bone Morphogenetic Proteins (BMPs)

Bone morphogenetic proteins are members of the TGF-β superfamily. BMPs were discovered by Marshall R. Urist in 1965. Since then 15 individual BMPs have been identified (Hollinger *et al*., 2005, p.130) and several including BMP – 2, -4, -5, -6, and -7

have been shown to be osteoconductive (Hollinger *et al.*, 2005, p.130). These BMPs stimulate differentiation of mesenchymal stem cells to an osteochondroblastic lineage. (Hollinger *et al*., 2005, p.130).

BMP-2 promotes apoptosis in primary human calvarial osteoblasts (Hollinger *et al*., 2005, p.130). BMP-3 is the most abundant BMP in demineralised bone and it may act as an important modulator of the activity of other osteogenic BMPs *in vivo*. In 2003, Campisi *et al.* (Hollinger *et al*., 2005, p.130) showed that BMP-2 and -4 were highly expressed in osteoblastic cells during distraction in a rabbit mandibular distraction model. They suggested that BMP could participate in the transduction of mechanical stimuli into biochemical response. In particular rhBMP-2 stimulates the activity of alkaline phosphatase in bone marrow stromal cells (Thies *et al*., 1992).

The osteoinductive properties of injectable BMPs into polymeric scaffolds was suggested by Saito N. in 2003, (Hollinger *et al*., 2005, p.131) and in particular rh-BMP-2 was found to successfully regenerate bone in critical-size defects in rats, rabbits, sheep and dogs (Hollinger *et al*., 2005, p.131). Yet, the application of BMPs in phylogenetically higher species remain questionable due to the superphysiological doses of rh-BMP-2 used (0.75 & 1.5mg/mL) in spinal fusion model in monkeys by Boden and co-workers in 1998 (Hollinger *et al*., 2005, p.131). Administration of BMPs in the amount of milligrams have raised serious concerns regarding the unpredictability of potentially sinister sequelae (Hollinger *et al*., 2005, p.131). Suggested therapeutic dosages of rhBMPs are presented on the following table:

SPECIES	**DOSAGE**
Human	1.5 – 3.5 mg (10^{-3} of gram)
Rats	10 μg (10^{-5} of gram)
Cell culture/ embryonic development	1pg (10^{-12} of gram)

Table 2.1 Relative rhBMP dosage in different species. The 10^{-x} values in the parentheses provide an idea of the concentrations of the chemicals necessary to induce a therapeutic result.

In order to initiate intracellular signaling, as a dimmer BMP binds to a complex of type I & II transmembrane receptors, consequently inducing a phosphorylation reaction and ultimately upregulation of bone-specific regulation genes.

Tissue Growth Factor Beta (TGF-β)

This growth factor superfamily is predominately found in bone, platelets and cartilage and their main function involves growth, differentiation and extracellular matrix synthesis. TGF-β receptors have been found in increased numbers on chondrocytes and osteoblasts which has lead researches to associate TGF-β with bone development and its repair process at all stages (Hollinger *et al*., 2005, p.129).

In 2003, Zhang and co-workers (Hollinger *et al*., 2005, p.130) showed that TGF- β1 enhances mineralization of human osteoblasts on implant materials and it has been well-documented as a potent chondrogenic factor, integral to chondrocyte and matrix homeostasis (Bosnakovski *et al*., 2006). *In vivo* experiments suggest that it might enhance the activity of BMP-2 (Hollinger *et al*., 2005, p.130). However, such results relied on the use of superphysiological doses of TGF- β1 preparation which raises concern about potential unwanted side effects in *in vivo* models. Overall the action of TGF- β, which initiates signaling similar to that of BMPs, is not well understood and it is speculated that it might not function alone as a bioactive factor in bone engineering.

Fibroblast Growth Factor (FGF)

FGFs, have been shown to produce promising results in promoting bone formation and enhancing the development of blood vessels. Marie *et al*., in 2002 (Hollinger *et al*., 2005, p.131) showed that FGF-2, FGFR-2 and BMP-2 are key factors in promoting proliferation,

differentiation and apoptosis in *in* vitro study on human calvaria osteoblasts. FGF-2 which is expressed in osteoblasts appears to be more potent than FGF-1 (Hollinger *et al*., 2005, p.132).

Insulin-Like Growth Factors (ILGF)

Insulin-like growth factors –I and –II (IGF) are produced by bone cells, stored in bone matrix and stimulate bone cell DNA synthesis and type I collagen production. *In* vitro and *in* vivo experiments have shown that IGFs stimulate osteoblast proliferation and differentiation (Hollinger *et al*., 2005, p.132). These growth factors act on osteoblasts inducing them to increase collagen production. They also inhibit collagen degradation by decreasing collagenase synthesis (Hollinger *et al*., 2005, p.132). Although IGF-II is the most abundant growth factor in bone it is IGF-I that appears to be the most potent of the two (Hollinger *et al*., 2005, p.132), with the latter being isolated from healing fractures in rats and humans (Hollinger *et al*., 2005, p.132). This local synthesis of IGF-I by osteoblasts appears to be important for bone remodeling. In particular this growth factor has been associated with intramembranous bone defect repair (Hollinger *et al*., 2005, p.133). When mesenchymal cells were transduced by IGF-I they preferentially migrated to the fracture site and repopulated the bone marrow, accelerating fracture healing (Hollinger *et al*., 2005, p.133). Overall, researchers have established the mitogenic effect of IGFs on bone marrow stromal cells although it appears that their effect on the differentiation depend on the maturation stage of these cells (Hollinger *et al*., 2005, p.133).

Platelet-Derived Growth Factors (PDGF)

In vitro studies have shown that PDGF, which is secreted by platelets during the early stage of fracture healing, is mitogenic for osteoblasts. However its therapeutic impact is yet to be established (Hollinger *et al*., 2005, p.133).

Vascular Endothelial Growth Factors (VEGF)

VGEFs are endogenously produced and promote angiogenesis, vasodilatation and increased permeability *in vivo* (Hollinger *et al*., 2005, p.134). These factors also induce endothelial cell proliferation, promote cell migration and inhibit apoptosis.

IN VIVO MODELS

Experimental animal models have been extensively utilized to test the efficacy and evaluate at a preclinical stage the appropriateness of novel structures, compounds and methodologies particularly in the field of bone engineering.

A number of general factors must be considered prior to choosing an animal model for such studies. These include the following:

1. Animal model appropriateness
2. Potential extrapolation to the clinical setting
3. Genetic homogeneity of the specific animal model
4. Available data on skeletal anatomy, bone physiology and biomechanical properties and osseous wound healing
5. Cost and availability of the model
6. Application of the results across species
7. Ease and adaptability of the model to experimental and laboratory manipulations
8. Ecological considerations
9. Ethical and societal implications

Specifically to bone engineering, the "goodness-of-fit" of a particular animal model will depend on the strategy employed to augment bony tissue. The levels of hypothesis testing are summarized on the following table. (Hollinger *et al*., 2005, p.219)

Bone Tissue Engineering Paradigms			
Level of Hypothesis testing	**Osteoconduction**	**Osteoinduction**	**Osteogenic Cell Transplantation**
Basic bone cell biology models	*In vitro* or *in vivo* manipulation of cell or tissue response to trauma using mechanical or environmental factors	*In vitro* or *in vivo* manipulation of cell or tissue response to trauma using growth factors, cytokines, or genes	*IN vitro* or *in vivo* manipulation of autologous or isohistogenic donor osteogenic cell response to host bone trauma
General clinical models	Repair of critical-sized defects using a passive mechanical scaffold	Repair of critical-sized defects using resorbable scaffolds seeded with growth factors, cytokines, or genes	Repair of critical-sized defects using resorbable scaffolds seeded with osteoblatsts or stem cells
Specific clinical models	Repair of bony defects in specific clinical conditions (e.g. periodontitis, diabetes, cleft palate, osteoporosis, etc.) using a passive mechanical scaffold	Repair of bony defects in specific clinical conditions (e.g. periodontitis, diabetes, cleft palate, osteoporosis, etc.) using resorbable scaffolds seeded with growth factors, cytokines or genes.	Repair of bony defects in specific clinical conditions (e.g. periodontitis, diabetes, cleft palate, osteoporosis, etc.) using resorbable scaffolds seeded with osteoblasts or stem cells

Table 2.2 Levels of Hypothesis testing in bone tissue engineering paradigms (Hollinger , *Bone Tissue Engineering,* p.219)

The animal models that have been used in the above levels of hypothesis in bone engineering include rodents (mice, rats, Guinea pigs, rabbits), dogs, sheep, goat, pig and monkeys.

Animal models for bone engineering of Critical-sized defects (CSDs)

One of the most important parameters in establishing the regenerative and osseo-inductive potential of osteogenic material is to apply them in defect areas where bone cannot be formed in adequate quantities to cover the entire size of the defect. The development of such a defect site is subject to the principle of *Critical-Size Defect*. Schmitz and Hollinger (1986) first defined a CSD as the "smallest size intraosseous defect in a particular bone and species of animal that will not heal spontaneously during the lifetime of the animal".

The anticipated physiologic response from the healing by secondary intention of a CSD is to histologically observe the formation of bony islands within the defect which hare joined by a characteristic fibrous connective tissue. This physiological state is known as bony non-union or fibrous union. More recently Hollinger and Kleinschmidt (1990) distinguished between a bony non-union from a CSD as a percentage of bone formed within the defect. They defined a CSD an area that "has less than 10% bone formation throughout its entire volume and any greater quantity of bone together with fibrous tissue comprises a bony non-union".

Developmentally the calvaria arise exclusively from intramembranous ossification. It has relatively limited vascular supply, poor healing properties and a biological inertness similar to that of long bone (Schmitz & Hollinger, 1986). The same group of workers indicated that in a period of 4 weeks even 3mm diameter defects in Sparague-Dawley rats had failed to heal completely.

Overall trephine calvaria CSDs tend to be more predictable in size and reproducible than CSDs in long bones (Davies, 2000).

MATERIALS AND METHODS

We obtained IACUC approval for our protocol and our laboratory facilities were approved by DLAM.

ANIMALS

A total of 23 male, 5 month old rats (Sprague-Dawley) were used for this experiment. The animals were purchased from Harlan, Inc., (Indianapolis, IN). The animals were individually housed in plastic cages in a monitored environment (22 ^{o}C, 12:12 hr light cycle). They had *ad libidum* access to drinking water and a standard laboratory rat food pellet diet.

SURGICAL PROCEDURE

Anesthesia was induced presurgically by intraperitoneal injection of ketamine/ xyalazine (40-80 mg/kg; 5-20mg/kg respectively). The toe-pinch and the eye reflexes were used to monitor adequate level of anesthesia during the surgical procedure. The animals were positioned in sternal recumbency and monitored for respiration rate, and toe-pinch and eye reflex throughout and after the procedure as a way to ensure an appropriate level of anesthesia. Immediately before surgery each animal was given a subcutaneous injection of buprenorphine (0.15 mg/kg; Henry Schein, Melville, NY) for post-operative analgesia, and an intraperitoneal injection of 5ml of normal saline (0.9% NaCl; Henry Schein) for sensible and insensible fluid losses during the operative and recovery period. The conjunctiva was

protected with the application of antibiotic ointment ("Perlube"). The incision site and wound area were shaved using an electric shaver and prepared with Betadine® scrub and 70% isopropanol. Using aseptic technique, a midline skin incision from the mid-nasal bone area to the posterior nuchal line was made and the underlying periosteum was incised and dissected. A trephine bur, with internal diameter of 8.0 mm and external diameter 8.9 mm, attached to a rotating slow-speed dental handpiece was used to create an 8.9 mm diameter defect in the bone. The dura was carefully guarded to avoid perforation and damage to the mid-sagittal blood vessels. The drilling site was under constant irrigation with a mixture of normal saline and lidocaine/ epinephrine in equal parts to minimize bleeding. Once the bone defect was prepared and the animal was stable, the implants were set in place. The implants were precut (diameter 8.0mm x 2.0mm thickness) absorbable collagen scaffold (Duragen®). At this point, sterilized test scaffold were saturated/ soak-loaded with either 1-2 drops of sterile 0.9% saline or an E-Matrix™ solution, or rhBMP-2 solution (5μg/ml) and placed in the defect. The surgical wound was closed by approximating the overlying tissues and suturing in layers with resorbable 5-0 Vicryl sutures (Ethicon, Somerville, NJ). Then, the animals were individually housed at room temperature and observed until they ambulated and did not show any visible signs of distress. After that, they were transferred to cages and were given access to water and food *ad libidum*. Approximately 8 hours after surgery each animal was given another subcutaneous injection of buprenorphine for post-operative analgesia. 24 hours after the surgery, each animal was given a subcutaneous injection of ketoprofen (5mg/kg; Henry Schein) in order to provide long-term analgesia. The animals were monitored daily for signs of complications related to surgery or illness. The animals were euthanized by CO_2 inhalation 2, 4 and 6 weeks after surgery. After euthanasia with CO_2, perfusion fixation was performed using 10% formalin and the craniotomy sites were recovered. After debriding of soft tissue, harvested tissues were placed in 10% formalin. The periosteum was maintained intact on the samples. For each of the timelines tested the animals were distributed as follows:

Test groups	# of subjects	Implant materials	Defect
Control	2	collagen & saline	8.9mm diameter on calvarium
Positive control	3*	collagen & rhBMP-2	
Test	3	collagen & E-matrix™	

* data available from only **2** subjects in the 2 week group

Table 3.1 Distribution of animals in experimental groups according to tested periods.

The study was conducted in non-blinded standards, as the surgical examiners were also involved in the histological analysis of the specimens.

RADIOGRAPHIC ANALYSIS

Radiographs of the rat calvaria gross samples were obtained to demonstrate defect size and the amount of mineralized bone within the defects. Standardized digital radiographic images were obtained using a dental radiographic unit (Gendex). Each of the specimens was rinsed with sterile water and excess fluid was removed. The specimens were individually positioned on a digital image receptor (27x36mm) at right angles to the source of the beam and were exposed to (66kVp, 8mA for 0.06 seconds). Densitometric tracing of the radiographs was used to estimate bone fill. The mean grey value (MGV) was calculated for each radiograph.

HISTOMORPHOMETRY

Excised samples were decalcified and bisected along a line parallel to the sagittal suture. The specimens were processed for regular histology. All paraffin-embedded specimens were sectioned at 5μm and the sections stained with hematoxylin and eosin (H&E). Using "Image J" software, the total defect and bone areas were measured. Only the areas of mineralized bone matrix and areas of osteoid were included. Areas of trabeculation were excluded. Those

two parameters and the area occupied by voids were measured in each of the three histological steps and the values averaged to obtain the specimen values. Individual specimen values were averaged to obtain group means and calculated deviations for defect, bone and void areas in mm^2. Group means and standard deviations were calculated for the percentage of the defect area occupied by bone in the microradiographs and the histological sections and for the percentage of the defect area occupied by voids in the histological sections. Goldner's trichrome staining was carried out on select slides for quantification of the osteoid production within the critical size defects.

Additional calvaria sections were further stained with Goldner's Trichrome Method. Stains were purchased from Electron Microscopy Sciences Inc. Once the paraffin sections were available they were treated and stained according to the following guidelines:

1. Deparafinise at 60.1^{o}C in block heater for 30 minutes.
2. Decerated in Xylene, twice for 2 minutes each time. they were then placed in absolute alcohol for 5 minutes each; 95% alcohol, 2 changes, 2 minutes each; then rinsed with distilled water. These steps were carried out by a dedicated apparatus (Slide Moat, Boekel, Boekel Scientific) in our oral pathology lab.
3. Mordant in *Bouin's Fluid* solution for 1 hour at 56^{o}C until formalin fixed.
4. Cool and wash in running tap water until yellow color disappeared.
5. Rinsed in distilled water.
6. Slides placed in *Weigert's Solution* for 10 minutes
7. Washed in running tap water for 10 minutes.
8. Rinsed in distilled water.
9. Stained in *Ponceau Acid Fuchsin* for 5 minutes.
10. Washed in *Acetic Acid, 1%.*
11. Placed in *Phosphomolybdic Acid-Orange G* solution until collagen was decolorized.
12. Rinsed in *Acetic Acid, 1%* for 30 seconds

13. Stain in *Light Green Stock Solution* for 5 minutes.
14. Rinsed in *Acetic Acid, 1%* for 5 minutes.
15. Section were blotted but not allowed to dry.
16. Dipped quickly in absolute alcohol
17. Slides were dehydrated in 95% alcohol and absolute alcohol 3 changes each. Clear in distilled water, 3 changes. These steps, too, were carried out in the Slide Moat apparatus.
18. Coverglass was mounted onto stained slides (coverslipping) once coverslip medium, (Permount) was applied (refractive index of 1.48-1.56)

The staining results were interpreted according to their color as follows:

Brownish black – nuclear chromatin

Bright red – cytoplasm

Orange – erythrocytes

Red – muscle, osteoid

Green – collagen, mineralized mature bone

STATISTICAL ANALYSIS

Our sample size (8 animals per timeline) was not adequate to warrant statistical analysis using ANOVA and t-testing. Thus, we restricted our analysis to descriptive statistics only using percentages of absolute values.

Studies measuring the delivery of BMP to calvaria defects measured a mean difference (δ) between a sham treatment and BMP loaded group of 1.51mm^2, with a standard deviation (σ) of 1.34 mm^2 for the experimental group. Using 9 animals per treatment group ensures that

with a 0.05 Type 1 probability error (α) the experimental power is 88%. We used one-way ANOVA to evaluate

1. whether there are any differences between different treatment groups within each time line
2. if for each treatment group there is any difference in the amount of bone produced between the 2^{nd}, 4^{th} and 6^{th} week time lines.

Where the p value in either of the above experiments indicated statistical difference (<0.05), a t-test was run to determine between which treatment groups (in one timeline) or which timelines (within a specific treatment group) the difference was significant for.

RESULTS

HISTOLOGY

Representative histological slides only were selected to demonstrate the progress of bone regeneration associated with each treatment group in the second, fourth and sixth week of assessment.

In all specimens the lamellar pattern of growth is defining the borders of the CSD. At two weeks out from the surgery date there are negligible areas of osteoid present in the control week group that can be found adjacent to the periosteum. The latter seems to be delineating the outer side of the defect. Most of the scaffold material (DuraGen®) appears to be relatively intact.

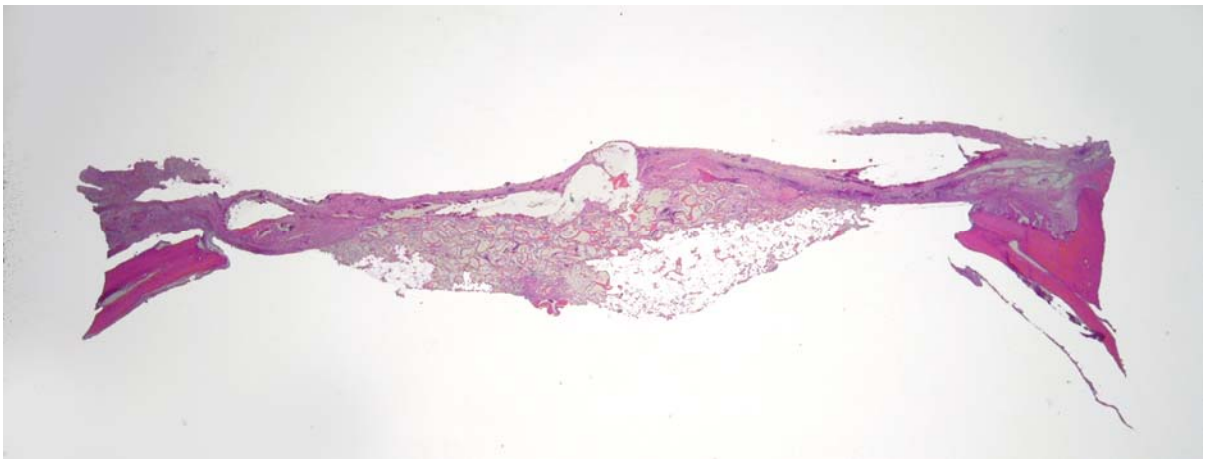

Figure 1. Control group (DuraGen® and saline) at 2 weeks.

In the E-matrix^{TM} group, there is also very little evidence of bone formation (Fig.2). The central area of the defect on this slide is associated with an inflammatory reaction consistent with the presence of the suture material (Vicryl, 4/0).

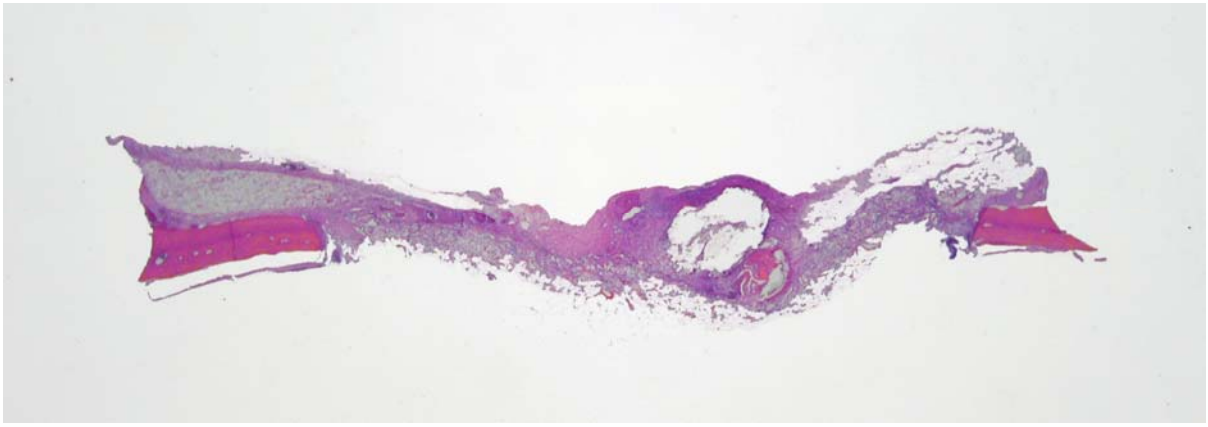

Figure 2. E-matrix^{TM} and DuraGen® at 2 weeks.

On the contrary osteoid formed fairly uniformly along the length of the defect in the rhBMP-2 group (Fig.3). The collagen scaffold (DuraGen®) has not yet been fully resorbed occupying a thin layer along the entire length of the defect on the **brain** surface of the defect.

Figure 3. DuraGen® and rhBMP-2 at 2 weeks.

At four weeks some osteoid has started forming in the central portion of this section in the control (Fig.4). Again, an inflammatory reaction is associated with the area of the suture material on the right side of the specimen in Figure.4.

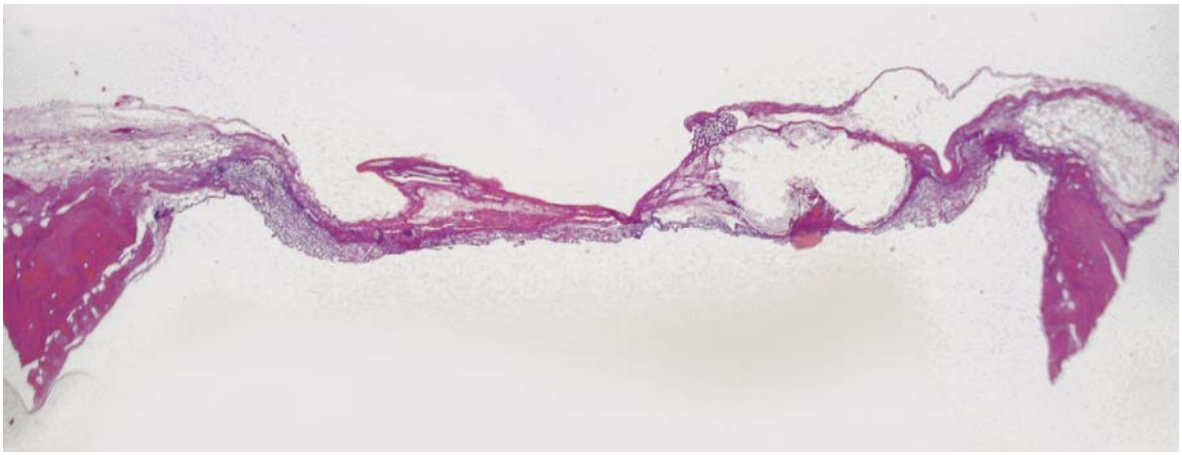

Figure 4. Control (DuraGen® and saline) at 4 weeks.

The section in Figure 5, which is representative of the bone repair pattern for the E-matrix™ group at 4 weeks, has not been taken through the widest portion of the defect but rather closer to the edges. Almost the entire length and half the thickness of the CSD is occupied by osteoid. Portion of this increased volume of bone might be due to the proximity to the periphery of the defect where osteogenesis commences during the reparative process.

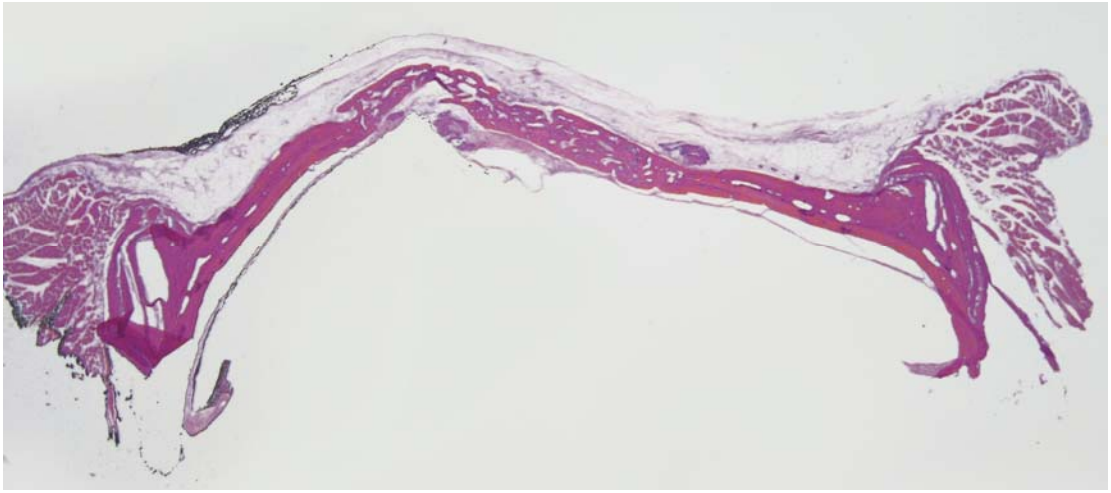

Figure 5. E-matrix™ and DuraGen® at 4 weeks.

In the rhBMP-2 group we can see a considerable amount of osteoid formation predominately peripherally. The central portion of the specimen in Figure 6 is associated with two features. The first is the inflammatory area related to the suture material. The second is the thinning of the thickness of the specimen right of the inflammatory portion. This could be either an artifact due to bending of the tissue slice when prior to its placement on the slide or stretching of the tissue when slices were being obtained. Another explanation is the presence of a tear in the collagen sponge (DuraGen®) during the implantation period.

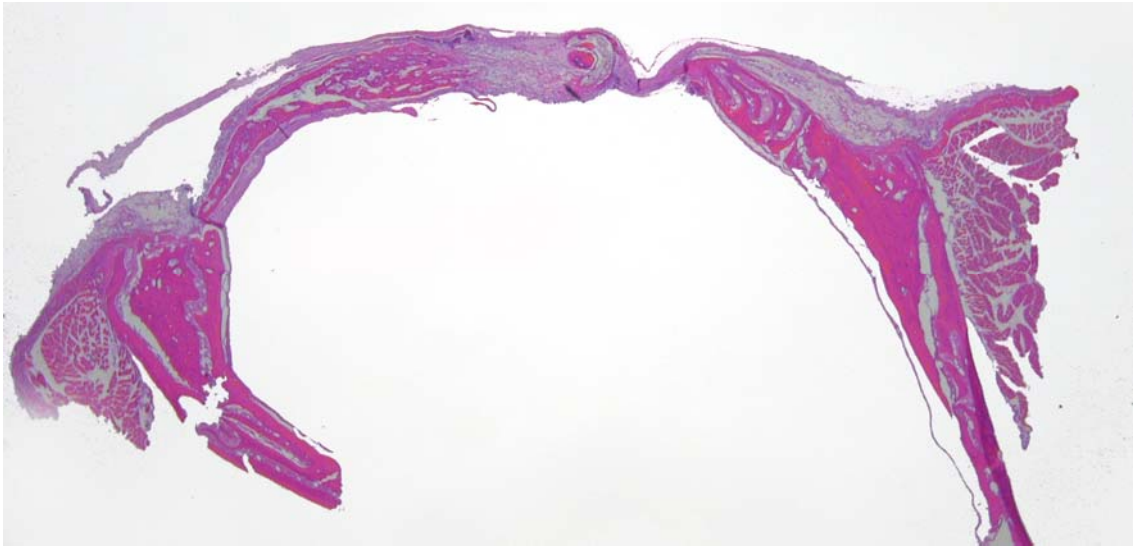

Figure 6. DuraGen® and rhBMP-2 at 4 weeks.

At six weeks in the control group (Fig.7) some osteoid has been sparsely formed along the CSD but most of the area is occupied by loose fibrous connective tissue.

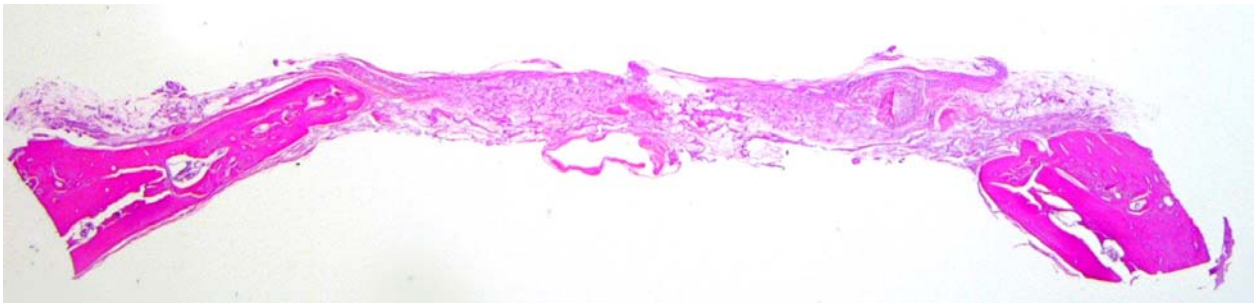

Figure 7. Control (DuraGen® and saline) at 6 weeks.

E-matrix™ induced a considerable amount of bone formation (Fig.8), which is thicker towards the edges of the CSD but lacks, however, in continuity along the entire length of the defect. In contrast to earlier timelines, the bone appears to have matured and become more organized. The presentation is consistent with that of woven bone. DuraGen® has completely resorbed.

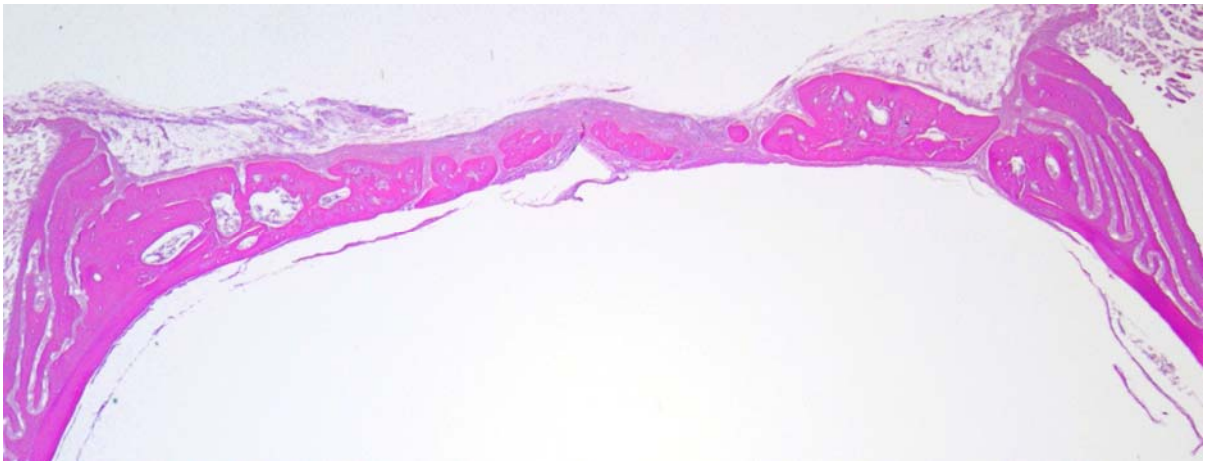

Figure 8. E-matrix™ and DuraGen® at 6 weeks.

In the rhBMP-2 group we also appreciated lack of continuity of the newly formed bone which too has the appearance of woven bone. There is some evidence of DuraGen® still being present on the **brain** side of the defect.

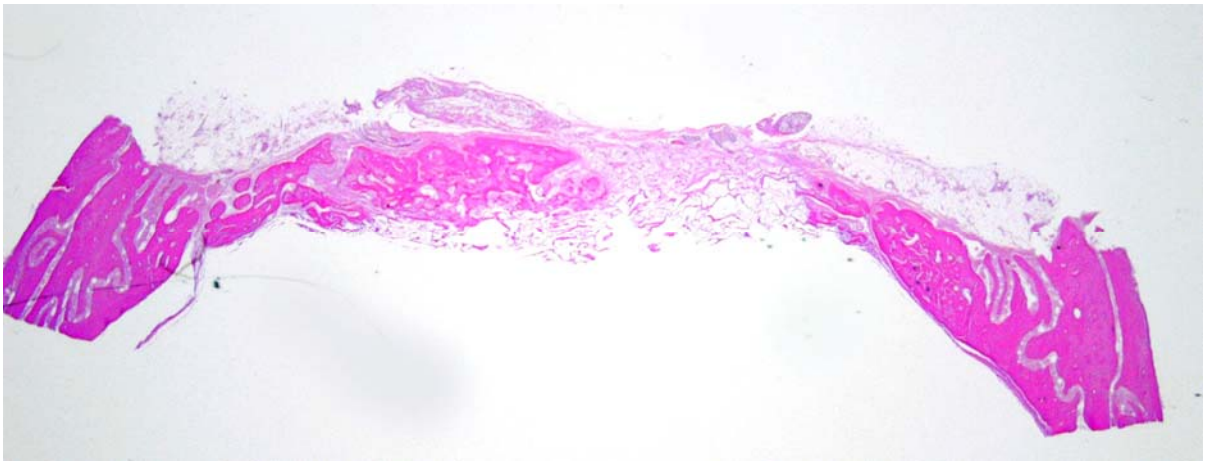

Figure 9. DuraGen® and rhBMP-2.

IMAGE J ANALYSIS

We used the “Image J” software for our histomorphometrical analysis. The periosteum was preserved on the specimens, thus providing the boundaries of our CSDs. Only the areas of woven bone and osteoid were accounted for. Any voids that could even be part of the trabecular bone pattern were excluded. “Image J” analysis was applied to individual slides. Specimen values were averaged to obtain group means and calculated deviations for defect, bone and void areas in mm^2. Group means and percentages were calculated for the percentage of the defect area occupied by bone in the microradiographs and the histological sections and for the percentage of the defect area occupied by voids in the histological sections. Table 4.1 presents the average percentage of area of the defect occupied by newly formed bone. For the complete account of defect area per each slide refer to Tables A.2, A.4 and A.6 in the appendix section.

Treatment	2 week	4 week	6 week
Collagen and saline	2.12	10.01	8.55
Collagen and BMP	26.20	42.61	22.12
Collagen and Ematrix™	5.08	40.21	22.12

Table 4.1 Average Percent (%) of bone formed within the defect.

Minimal amount of area of the CSD was occupied by bone in 2 weeks in the control (2.12%) and E-matrix™ (5.08%) groups. In contrast to those values we observed a marked production of bone, covering 26.20% of the CSD, in the rhBMP-2 group.

However, 40.21% which was reduced to 22.12% of the CSD was occupied by osteoid in the E-matrix™ group in the 4 and 6 weeks timeline respectively. Newly formed bone induced by rhBMP-2 filled almost exactly the same portion of the defect as that in the E-matrix™ group

for the same timelines. The corresponding areas of osteoid formed by the control group were consistently low to about one third of the value shown by the other two experimental groups. These values are graphically presented in table 4.2.

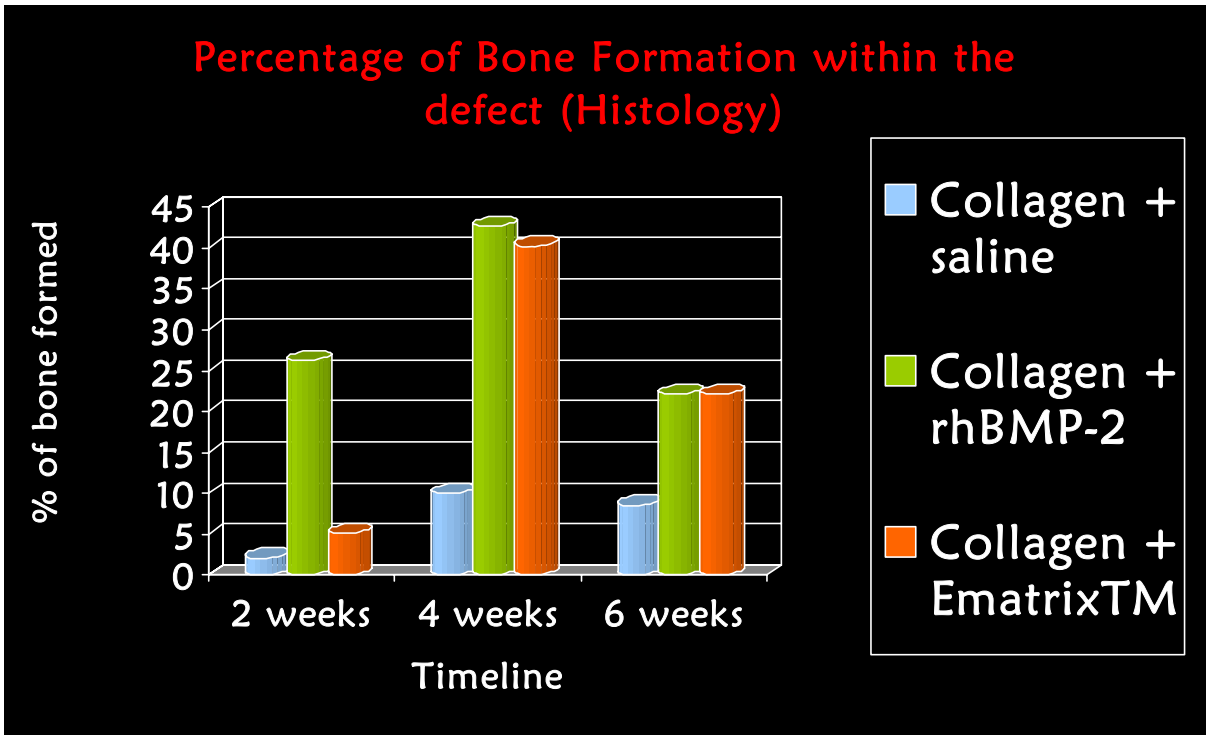

Table 4.2 Graphical representation of the average percentage of bone formation within the defect.

RADIOGRAPHY

As with the histological analysis, we chose to include representative radiographs of each tested group in each of the three timelines.

In the 2 week timeline, there is little to no evidence of bone formation in all groups (Fig. 10, 11 & 12). Although some osteoid formation is suggested from the histomorphometric analysis in the rhBMP-2 group, it cannot be accounted for in the representative radiograph (Fig. 12). The radiopacity in all three radiographs at this stage are attributed to the DuraGen® scaffold.

Figure 10. Control at 2 weeks. **Figure 11.** Ematrix^{TM} at 2 weeks. **Figure 12.** rhBMP-2 at 2 weeks.

At four weeks the DuraGen® scaffold appears to have been completely resorbed in the control group (Fig.13). In the E-matrix^{TM} group (Fig.14), however, we can appreciate that a considerable area of the defect is occupied with osteoid/ woven bone especially around the periphery. Evidence of newly formed bone is present also in the rhBMP-2 group peripherally as well as centrally within the CSD.

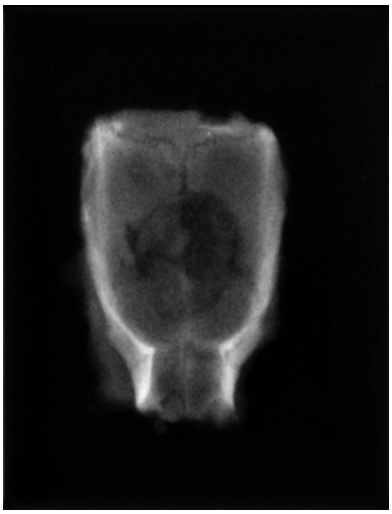

Figure 13. Control at 4 weeks. **Figure 14.** E-matrix^{TM} at 4 weeks. **Figure 15.** rhBMP-2 in 4 weeks.

Finally, at six weeks new bone begins to form even in the control group but only peripherally (Fig.16). Comparable areas within the defect have been occupied with new bone both in the E-matrix^{TM} and rhBMP-2 groups (Fig. 17 & 18). These areas are considerable larger than those in the control group and they are arranged in a centripetal fashion at the centre and periphery of the CSDs.

Figure 16. Control at 6 weeks.

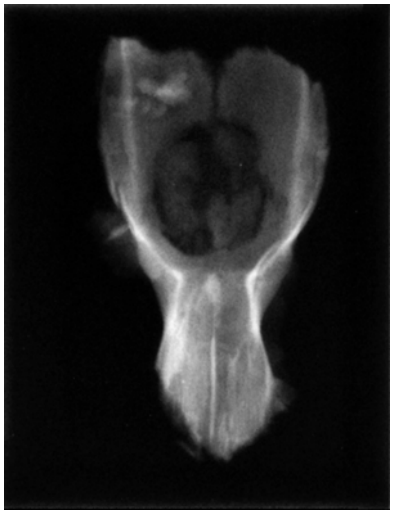

Figure 17. Ematrix^{TM} at 6 weeks.

Figure 18. rhBMP-2 at 6 weeks.

Due to errors in the measurement of the amount of bone formed in the defect area the MGV calculations thereof were discarded.

GOLDNER'S TRICHROME

This staining method was used to differentiate visually the areas of osteoid, woven and lamellar bone as well as collagen present in our specimens. Intense red denotes mineralized bone (woven or mature lamellar bone) and the light blue interprets areas of either osteoid (unmineralised bone matrix) or collagen which can be easily differentiated due to their distinct architecture.

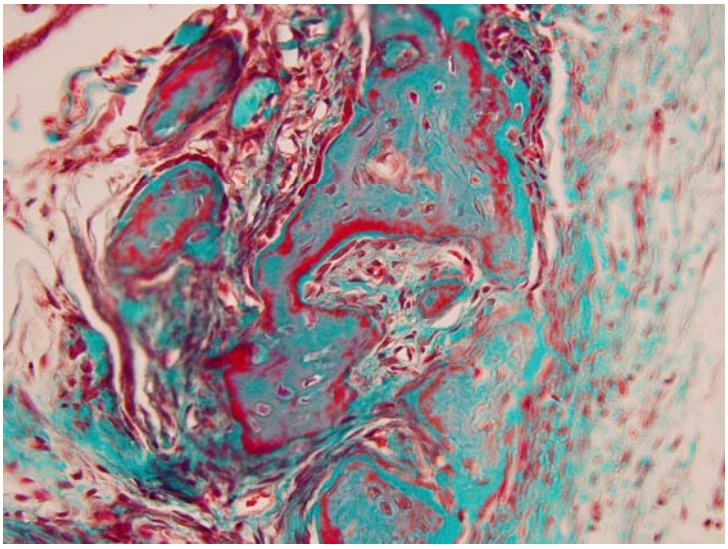

During the early stages of bone repair, we can appreciate the abundance of connective tissue with its wavy presentation (blue). There is very little osteoid and woven bone produced at this stage.

Figure 19. Early stage in bone repair (2 weeks, control).

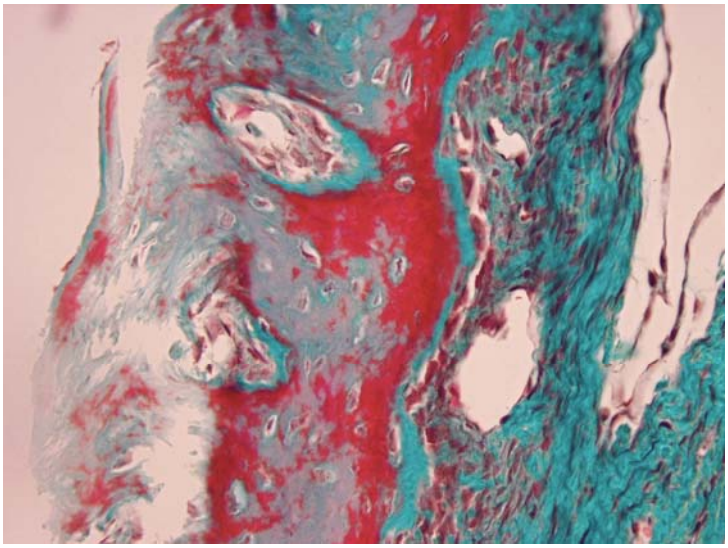

Specimens showed a marked increase in the amount of new bone produced at 2 weeks in the rhBMP-2 group. The trichrome staining confirmed the increased production of woven bone and showed evidence of osteoblastic rimming laying osteoid (blue) between them and the woven bone area.

Figure 20. Early stage in bone repair (2 weeks, rhBMP-2).

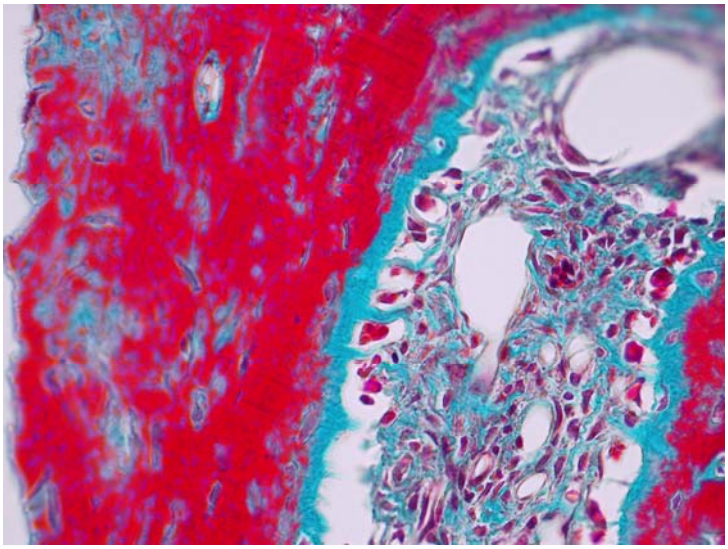

In the later stages of bone repair there is a marked increase in the amount of woven bone containing osteocytes. Osteoblastic rimming is still evident by the presence of cuboidal cells next to actively forming area of osteoid (blue).

Figure 21. Late stage of bone regeneration (6 weeks) (rhBMP-2).

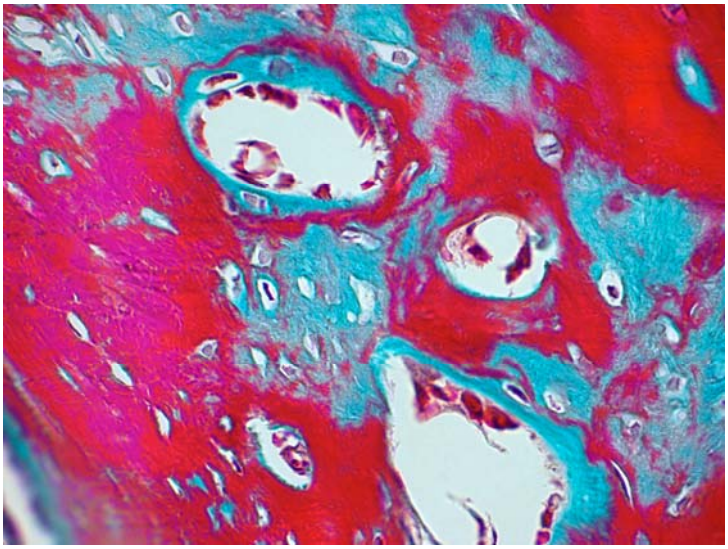

Consequently the newly formed bone acquired a more organized and mature architecture compared to the one present in the earlier stages of osteogenesis. Lamellar bone structure can be seen on the left side of this figure (Fig. 22). Haversian canals have also begun to form.

Figure 22. Late stage of bone regeneration (6 weeks) (E-matrix^{TM}).

DISCUSSION

Re-examination of experimental design

In this experimental model we assessed the potential of bone regenerative capability of a naturally derived polymer, E-matrix™ (porcine collagen + gelatin), on a true Critical Sized Defect (CSD) in rats. After 6 weeks of healing period, 22.12% of the original CSD area showed new bone formation whether it was treated with rhBMP-2 or our proprietary material, E-matrix™. The histological results for E-matrix™ were particular encouraging with respect to the organization and quality of the newly formed bone. The latter appeared to be of highly comparable architecture to that seen in bone formation during repair process by secondary intention.

The organization of the newly formed bone as it appeared on the histological examination as well as the potential biomechanisms that lead to its production will be discussed later in this chapter.

It is worth noting the pattern of bone formation that transpired between the fourth and sixth week of observation irrespective of the type of treatment. There was a decrease in the area occupied by the newly formed bone. Such reduction can be explained by the physiology of bone remodeling. The resorptive phase of bone remodeling occurs between

Carrier

In our study we used a pre-formed disc-shaped synthetic collagen matrix (Duragen®, Integra™) as a supporting scaffold to deliver a novel hydrogel scaffold onto critical-size calvaria defects in rats. According to the manufacturer, DuraGen® has been predominately intended for dural defect closure and overall for neurological defect repair. Rabinowitz *et al*.,

(2005) studied the effect of this material by *in vitro* by culturing dissociated rat cerebral neurons on poly-L-lysin and cryostat-sectioned Duragen®. They concluded that DuraGen® has no adverse effects on the survival or process growth of neurons and thus it is safe to use as a dural substitute. In a comparative *in vivo* study in suboccipital craniotomy in humans between two alternative dural substitutes (DuraGen® and AlloDerm), Danish *et al.,* (2006) concluded that both materials are acceptable scaffold materials with DuraGen® exhibiting much shorter healing time than AlloDerm. Cerebrospinal fluid containment was proved to be successful by Narotam and co-workers (2004). In a retrospective study of 110 patients that had undergone spinal dural repair and regeneration they concluded that cerebrospinal fluid containment was successful in over 95% of the cases.

Although there was no macroscopic evidence of dural perforations during the rat surgeries in our experiment, the use of DuraGen® as our basic scaffold at least ensured effective closure against any accidental dural perforation and consequent possibility of CSF leakage.

In addition in our study there was no histological evidence of any inflammatory reaction associated with DuraGen® and none of the tested subjects developed infection as a consequence of their treatment. Due to the type and site of induced experimental calvarium defect we felt that DuraGen® was the most appropriate semi-rigid scaffold.

The scaffold material under investigation, E-matrix^{TM}, belongs to the wider category of hydrogel scaffolds. Where solid scaffolds provide a substrate upon which cells may adhere, liquid and gel scaffolds function to physically entrap cells and osteogenic molecules (Elisseeff *et al*., 2005).

Yet, researchers have been looking into modifying hydrogels in order to introduce adhesive properties to them. Nguyen *et al.*, (2003), observed increased adherence of osteoblast-like Human Osteosarcoma (HOS) cells *in vitro* when inorganic bone mineral (ABM) particles coated with P-15 peptide (cell-binding domain of type-I collagen) (PepGen^{TM} P15®, *Ceramed*) were suspended in injectable hyaluronate hydrogel. As a result of improved

adherence the following phenomena were observed: increased cell migration and cell coverage on the ABM surface; increase in the quantity and presence of stress fibers; enhanced gene expression which promoted considerable deposition of mineral matrix. In the work of Rowley and co-workers (1999), alginate was shown to have the potential of a model synthetic extracellular matrix when its properties were modified with the addition of RGD-containing cell adhesion ligands. Alginate and other hydrogels are able to discourage protein adsorption due to the hydrophilic nature of their polymers. (Smentana, 1993).
Passos-Bueno *et al*. (1999) utilizing a monolayer of hydrogel as a scaffold, cultured osteoprogenitor and MCS from mice with Apert Syndrome. Successful outcome suggested that in view of the cell behavior in the hydrogel the latter could be used to evaluate tissue development and potential therapeutic applications. Sweeney *et al.* (1995) noted that purified type I collagen gel matrix alone induced rapid and total CSD repair in rats. Reddi (2000) observed that type I collagen binds bone-promoting growth factors of the TGF family (including TGF-β and BMPs). This could mediate migration of osteoprogenitor cells into the defect, further promoting osteogenic proliferation and differentiation.

E-Matrix™

According to the manufacturers E-matrix™ is a biologically active co-polymer that stimulates fetal-like wound healing. E-Matrix is unique in its ability to promote this rapid, nearly scarless healing process normally found only in early fetal development. As a result, E-Matrix treatment rapidly heals chronic ulcers recalcitrant to other conventional and experimental treatments.

E-Matrix Structure

E-Matrix is a co-polymer of a high molecular weight protein and a high molecular weight carbohydrate designed to mimic early fetal mesenchymal connective tissue. This fetal

mesenchymal tissue is composed primarily of single stranded molecules as opposed to the triple stranded configuration found in the adult. The E-Matrix protein moiety is derived from triple stranded collagen extracted from adult porcine skin and processed into an open, monomeric single stranded form. In this monomeric configuration, polar binding sites are exposed that are unavailable in the native triple stranded configuration of adult collagen. This open configuration with exposed polar groups is maintained by co-polymerization with the high molecular weight carbohydrate. Enhancers are added to maintain this configuration during manufacture and storage.

E-Matrix Mechanism of Action

E-Matrix is a bioactive film that binds to host cells responsible for initiating the wound healing response. It is this physical interaction between E-Matrix and the host cells that initiates the wound healing cascade. Polar sites on the host cells are exposed through the disruption caused by the injection process and E-Matrix binds to these polar groups. In vitro studies with human fibroblasts have demonstrated E-Matrix binding to cell surfaces and the resultant cell aggregation. This interaction between E-Matrix and the cell surface in turn alters the gene expression of these cells. One of the genes that E-Matrix up-regulates is Transforming Growth Factor beta 3 (TGF beta 3), which is believed to be involved in the fetal-like wound healing response. It is hypothesized that the E-Matrix alteration of gene expression in appropriate host target cells activates the fetal-like wound healing response in treated wounds.

Biological Effects of E-Matrix

Fetal wound healing is characterized by an altered pattern of response compared to adult wound healing. Hallmarks of the fetal response include: a less tightly cross-linked extra-cellular matrix; less differentiated cells in the wound bed; reduced wound contraction; rapid and sustained neo-vascularization; and scarless wound healing (Samuels and Tan, 1999). In

pre-clinical studies, E-Matrix has been shown to alter the type of extra-cellular matrix produced in the healed wound bed from a highly cross-linked, dense structure normally found in healed adult wounds to a more open reticular structure found in healed fetal wounds. E-Matrix treatment produces cells in the wound bed that are "mesenchymoid" in morphology and not the differentiated myofibroblasts typically seen in adults. As a result, there is less wound contraction as reflected by significantly reduced levels of the contractile protein actin (smooth muscle specific actin, SMSA) in the wound bed. E-Matrix also improves the vascularity in the injected areas and this vascular response is sustained in contrast to the transient increase in vascularization seen with growth factors. As a result of this fetal-like pattern of healing, wounds treated with E-Matrix heal with significantly reduced scarring and full integration of the tissue with existing host tissue. The tissue regeneration that results from E-Matrix treatment has now also been observed in patients with diabetic foot ulcers recalcitrant to other therapies

Intellectual Property

Encelle has developed a strong intellectual property position with respect to its technologies. Work to date has resulted in thirteen patents which have been issued and seven that are pending at the United States Patent and Trademark Office (USPTO).

Patent applications claiming E-Matrix have been filed and are being prosecuted in all major markets (U.S., Europe, Japan, etc.). Filed claims include E-Matrix formulation, broad mechanisms of tissue regeneration, methods for increasing vascularization and promoting wound healing, and methods for medium and matrix for long-term proliferation of cells.

Osseoinductive agents

rhBMP-2 served in our experiment as the “gold standard” for bone formation. Originally this protein was identified as BMP-2A by Wozney *et al*., in 1988 and it possessed one tenth of

the bone-inductive potential of the pure native bovine protein when reconstituted with inactive, insoluble collagenous bone matrix and assayed ectopically in rats (Wang *et al*. 1990). Since then rhBMP-2 were further modified and shown to stimulate *in vitro* the activity of alkaline phosphatase in bone marrow stromal cells (Thies *et al*., 1992). Other researchers showed in addition that rhBMP-2 stimulate pluripotent, non-osteogenic cells (Katagiri *et al.,* 1990) as well as cultured osteoblasts and osteoblast precursor cells which indicate the ability of the preparation to direct cell differentiation toward the osteoblast phenotype and the potential of genetically engineered rhBMP-2 to regenerate bone *in vivo* (Marden *et al.*). BMPs are the only known inductive agents. (Lind, 1996) and there is evidence that these molecules as well as TGF-β collaborate with to induce osteoblastic activity (Nguyen *et al*., 2003).

Concerns have been expressed with respect to increased dosages associated with the therapeutic effect of rhBMP-2. However, Poynton *et al.* (2003) defended the good safety profile and low systemic toxicity of BMP. It is worth noting that BMPs in general have a very high metabolic turnover and a half life of only few seconds once introduced to the defect site.

The rapid metabolism of BMPs unveils the need for the prolonged presence of these molecules in the sites of desired bone regeneration. Schmoekel *et al*. (2004) showed the potency in induction of bone regeneration in a CSD in the rat calvarium with a prolonged BMP-2 retention achieved using a fibrin scaffold. BMPs bind to bone ECM by interaction of heparin-sulphate proteoglycan (Ruppert *et al*., 1996) and to collagen types II and IV (Sieron *et al.*, 2002). This might be a valid consideration since we observed a rapid increase in the osteoid formation in our project in the rhBMP-2 group which was followed by a less prominent increase between the second and fourth week of observation.

Type of defect

The rat craniotomy defect is a convenient model for studying the bone regenerative potential of materials because of the ease of accessibility and the lack of requirement for fixation. CSD in this animal model are reproducible and have been tested in various *in vivo* studies

Rats have an accelerated bone metabolism and are able to spontaneously regenerate proportionally greater bone defects than humans (Davies, 2000). Thus, the use of this model and especially of mature rats in bone engineering does not warrant transferability of healing patterns and overall results to human. In addition, due to reduced bone growth and remodeling in aging populations, successful tissue-engineering procedures observed on immature animal models does not reflect the osteogenic properties of the tested biomaterial in adults (Davies, 2000).

Histological Results

Although H&E staining was run for initial histological evaluation, Goldner's Trichrome staining was selected as an additional histological assessment. This type of staining permitted the direct visualization of the areas occupied by osteoid and mineralized matrix which enhanced a crude observational assessment/ visualization of the amount of potentially new bone that was regenerated in our tested groups.

Unfortunately, the possibility of using an alternative staining method (von Kossa) was not an option since all our initial histological specimens had been decalcified at an earlier stage.

We found that it was essential to maintain the periosteum intact at the defect site in order to determine the exact dimensions of our CSD. The importance of this principle was also supported by Narang and Laskin (Davies, 2000). The presence or absence of the periosteum at the defect site is a key parameter when establishing the CSD for a particular animal model. The same authors showed that the size of a CSD on the fibula of Holtzman Albino rats

dropped from 12mm to 6mm when the periosteum was removed. They concluded that the presence of periosteum acted as a barrier to the defect site excluding its colonization by soft tissue and as a source of osteogenic MSCs thus promoting bone growth.

Radiographical Analysis

Assessment of bone formation on the radiographs using the Mean Gray Value (MGV) is inconsistent and unreliable. For the purposes of measuring the MGV the dura matter and the periosteum were left intact, defining the limits of the defect. However the similarity between their radiopacity and that of the newly formed bone, masked the areas of were bone was formed.

Pryor *et al*., (2005) assessed the effect of PRP therapy in inducing bone formation utilizing a 6.0mm diameter defect on rat calvaria. The assessment relied on radiographic observations of the specimens after 4 and 8 weeks of healing periods. The gross specimens were irradiated at 70kVp, 7mA for 0.083 seconds allowing 12 inch distance between the specimen and the x-ray source. The classification of the defects followed an elementary distinction in 3 groups based on 1. Non-closure, 2. Partial closure and 3. Complete closure of the defect area. The authors concluded that PRP preparation on ACS carrier had no significant effect on osteogenesis in their experimental model.

Yet, such a radiographic analysis appears to be a relatively crude method of assessment of bone formation that might be used as an adjunct to histological analysis. To our opinion the use of radiography can be justified in our experiment to provide a general outlook to a novel material's biological effect but not to draw final conclusions.

POTENTIAL MECHANISMS OF ACTION

Signaling via cell transduction/ Osseoconduction

Wilson-Hench (1987) suggested that osteoconduction is the process by which bone is directed to conform to a material's surface. In osteoconduction bone grows on a surface. This definition requires the presence of a scaffold or *osteoconductive* surface onto which bone is allowed to grow. The safest way to determine if a substance is osteoinductive is to inject it at a heterotropic site and analyze any potential bone formation.

Part of the reparative and remodeling process of skeletal tissue, which applies to our research model, is the early deposition of collagenous matrix. Subsequently, reparative cells from the defect borders migrate onto this matrix, organize and remodel the matrix through cytoskeleton and matrix synthesis/ degradation. Since the maintenance of the extracellular bone matrix is the primary goal of bone remodeling one can appreciate the importance of the presence of osteblasts and osteoclasts for the repair and homeostasis of the tissue.

Equally important for the survival of most cell types is their anchorage to the scaffold as this is a strict requirement for several functions such as migration, proliferation, differentiation and apoptosis (Rowley *et al*., 1999). Thus, we can hypothesize that E-matrix^{TM} possessed some inherent cell adhesion properties that potentially played a role in mediating and promoting recruitment of osteogenic cells (osteoconduction) from the defect's tissue boundaries.

Osseoinduction

Osseoinduction is a process commonly encountered upon new bone formation. As a biological process it implies the recruitment of primitive, immature and undifferentiated cells and their stimulation to develop into preosteoblasts.

BMP are the only known molecules with osseoinductive capacity and are released in response to trauma and bone remodeling (Ling, 1996). According to Frost (1989) the

inevitable injury sustained by the bone, marrow and soft tissue initiates the subsequent repair by sensitizing different types of surviving cells.

The rational behind the use of this material is based on the notion that an unidentified compound/substance intrinsic to E-matrix^{TM} is responsible for its osteogenic potential.

Another possible speculation is that this material's osseoinductivity may be due to its ability to modulate signaling pathways ultimately making cells more sensitive to osteogenic factors secreted in the defect area following trauma. Potentially the porcine collagen component in E-matrix^{TM} can alter the activity of protein kinase C and increase cAMP level in response to parathyroid hormone (Nguyen *et al*., 2003). PTHrP and PTH are secreted as serum ionized calcium falls. Both hormones stimulate osteoclasts and rapid resorption by directly stimulating osteoblast action which then mediates the ostaoclastic activity.

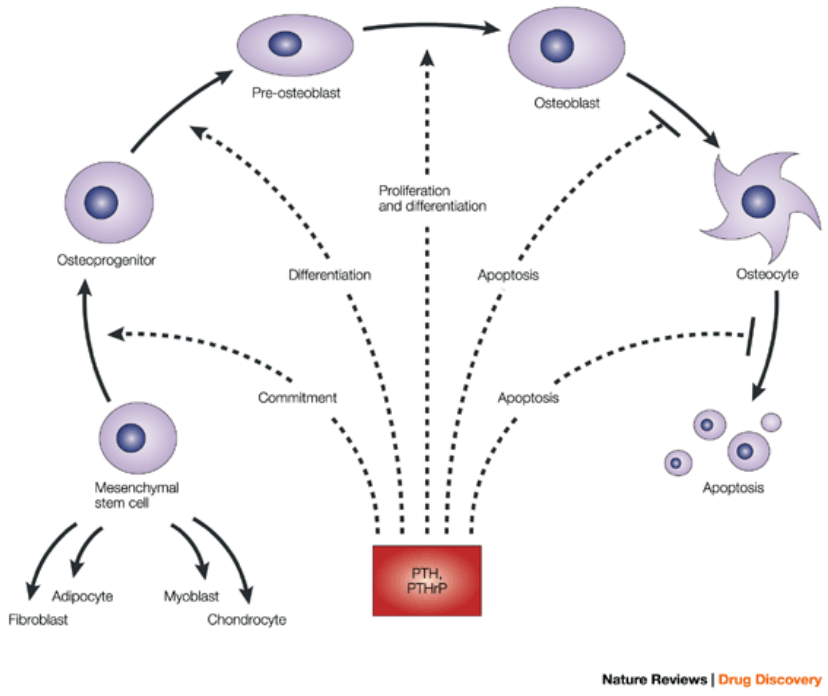

Figure 5.1: Effect of Parathyroid Hormone (PTH) and Parathyroid Hormone Precursor (PTHrP) on the differentiation process of mesenchymal and osteoprogenitor cells.

A reduction/loss of bone was observed in the E-matrix group between the 4 and 6 week group. This is attributed to the physiology of bone healing. Bone physiology dictates that the resorptive phase of bone remodeling commences 3-4 weeks following insult to bone.

VALIDITY OF THE MODEL

We tested our novel material on an established critical size defect. Such defects have been defined as "defects that show less than 10% of bone healing within the life of the animal" (Hollinger & Kleineschmidt, 1990). Thus, the production of bone that covers more than 10% of the defect area proves the osseoinductive properties of the material.

The rat as an animal model is an acceptable one for initial *in vivo* testing of a novel material and potential large number of subjects can be used for a valid statistical analysis.

Our data suggest that E-matrix^{TM} supports or promotes osteogenesis in the rat model. However the behavior of this material in large, space filling models e.g. tibia, mandible requires further investigation.

E-matrix^{TM} has been successful in human clinical trials for chronic skin wounds and has received FDA approval. Thus, it is poised for translational studies concerning bone repair.

ADVANTAGES OF THE TECHNIQUE

E-matrix^{TM} is a synthetic material utilizing a denaturated, high MW protein derived from porcine skin and high MW carbohydrate. Due to its nature and method of manufacturing it has reduced risk of disease transmission.

The material under investigation is biocompatible. There was no evidence in our histological analysis indicative of any adverse or inflammatory reaction associated with E-matrix^{TM}. A

reason for this could be the naturally occurring polymers which in a denatured state may be relatively non-immunogenic.

The cost effectiveness of using this material is marked. Compared to the considerable cost of using rhBMP-2 for its osseo-conductive properties, E-matrix^{TM} provides an alternative therapeutic option at a twentieth of the cost of BMPs.

E-matrix^{TM} exhibits synergism when used with other scaffold material such as HA/TCP, anorganic bone and membranes.

DISADVANTAGES OF TECHNIQUE

E-matrix^{TM} exists as a viscous gel in room temperature but its viscosity dramatically decreases at 38^{o} C. This physical property makes it a poor candidate for large, non-contained defects or areas that anatomically sustain increased loads, e.g. tibia.

As seen on the histological slides there is no evidence of this material being present even 2 weeks following its implantation. We speculated that E-matrix^{TM} is resorbed 3-5 days after implantation to the defect side. Ideally such material should have a sustained presence within the defect for at least 2 weeks for more prominent bone formation.

As this is the first *in vivo* study testing the osseoinductive properties of the material, it requires complete clinical documentation.

Another disadvantage of this technique from a clinical application standpoint is the surgical intervention in order to deliver the osteogenic material. However, if used as an injectable material within a contained space this relative disadvantageous point can be eliminated.

POTENTIAL CLINICAL APPLICATIONS

In the future, bone regeneration can be applied clinically where lack in bone mass can compromise or prohibit optimum treatment or when prognosis of final treatment is enhanced. Thus functional replacements for damaged or pathologic tissues can be made[11] for example in recreating missing osseous structures (vertical bone loss), correcting craniofacial deformities and enhancing bone/tooth or bone/implant functionality and long-term stability[12]. E-matrix™ was tested to be successful in regenerating bone in a non-loading area, the calvarium. The most applicable clinical situation for this type of material with promising results and particular interest to us is the craniofacial region. Due to functional and anatomical differences the craniofacial skeleton is divided to upper and lower facial skeleton. Where the main function of the latter is primarily occlusal, the cranial portion exists as a static edifice protecting the brain and organs of special sense and providing a foundation for the attachment of the musculature and overlying soft tissue involved in facial expression and masticatory function. As a result of the distribution of muscle attachments in this area there is relatively little direct force of impact and significantly less direct muscular force applied to much of the upper facial skeleton. In addition, the constraining forces of the overlying soft tissues affect the net force on the facial skeleton and thus warrant special consideration in that part of the skeleton where projection and fine contour are of significance (ch.50). Thus it is the restoration of the defects and asymmetries of the facial skeleton to their normal form that is the main goal of the craniofacial surgeon.

At this stage it is important - for the success of the regeneration and reconstruction of the facial skeleton - to appreciate the need for a rigid scaffold in order for the latter to withstand the overlying soft tissue compressive forces. Biological requirements of the upper facial skeleton augmentation in particular dictate volume maintenance from the scaffold and the ability for it to be molded into the fine contours of the regional anatomy. Terheyden et al. reported the ectopic formation of mass tissue (mandible) using a mesh as a rigid scaffold and rhBMP-2 as his osseoinductive agent to regenerate a mandible. Once the bone tissue on the

graft was mature it was transferred to the recipient site. Maybe such mass tissue culture and transfers that requires the property of osseoinduction from the grafting components can be a possible niche for the application of our tested proprietary hydrogel in the future.

The amount and quality of bone have been stated as some of the most important factors in the long term success of endosseous implants especially where augmentation procedures are required. Due to its potential superior performance in regenerating bone *de novo* this material can be considered in the application of alveolar ridge augmentation, sinus lift augmentation and even extraction site preservation following exodontia.

LIMITATIONS

One might also claim that there was no opportunity for osteoconduction due to the discrepancy between the defect size (8.9mm) and the scaffold size (8.0mm). Yet, the addition of the tested substances saline/hBMP-2 solution/Ematrix caused the collagen sponge to swell thus minimizing the distance between the implant and the margins of the defect. As a result of this there might have been no opportunity for osteoconduction between the borders of the defect and the grafted area due to the discrepancy between the defect size (8.9mm) and the scaffold size (8.0mm).

All specimens collected for histological analysis were decalcified prior to being stained with Eosin and Haematoxylin. Thus no slides were available to be subjected to the Von Kossa staining method. Differentiation between mineralized mature bone, osteoid and collagen would have been clearer had we been able to use that method. VonKossa staining would have also negated the need for Goldner's Trichrome staining.

Unfortunately we did not dispose an adequate number of animals in this pilot study to be able to run any statistical tests with reliable results for the data we collected from the histological

analysis. At this point we relied on descriptive statistics (percentages) to essentially observe the trends associated with our results.

The assessment of bone formation in the harvested calvaria areas via digital radiography and quantification using the Mean Grey Value (MGV) was problematic. The periosteum was left intact, defining the limits of the defect site, with only the soft tissues and brain matter being removed from the specimens. However, the radiopacity of the periosteum appeared to be similar to that of the newly formed bone, thus, masking the areas where new bone had been produced. For this reason we decided that the radiographic images would be used for the crude inspection of the area the new bone occupied in the defects.

SUGGESTIONS FOR FUTURE RESEARCH

One could propose to manufacture a cross-linked hydrogel in order to eliminate need for use of a rigid scaffold/ carrier. As a consequence this type of cross-linked/self-hardened/ photopolymerized scaffold will necessitate *in vitro* assessment to prove the lack of any harmful effects from the hardening process.

Further projects will need to be undertaken to establish biocompatibility of our novel material to sustain adherence and growth of cultured stem cells when the later are intended, once expanded in culture, for delivery to the defect sites. Potentially the presence of adhesive peptides allows for a more natural environment for the anchorage-dependent osteoblast, hence, mineral deposition by the osteoblasts would be increased (Burdick & Anseth, 2002).

To move a step forward towards the clinical application of such an osseoinductive material research need to be conducted on a higher primate animal model. In addition a larger number of subjects must be utilized to produce statistically significant results.

CONCLUSIONS

Within the limitations of these experiments, the following can be concluded:

(1) Ematrix^{TM} induces bone formation in rat calvaria Critical-size defects.

(2) The amount and histological appearance of the bone formed is comparable to that induced by rhBMP-2 over the same period of time.

(3) Further clinical documentation is necessary to establish osseo-inductive properties of the material.

APPENDICES

The statistical data presented in this study are numerical averages of the original data and their percentages. Considering the simplicity of these calculations there are no complex calculations to be presented in this section.

A. IMAGE J ANALYSIS

2 week group analysis

TREATMENT GROUP	SPECIMEN/ SLIDE NUMBER
Control (DuraGen & saline)	1, 2
Ematrix™ (DuraGen & Ematrix™)	3,4,5
rhBMP-2 (DuraGen & rhBMP-2)	6, 8

Table A.1 Distribution of animals (their identifying number) into the experimental groups at 2 weeks.

Animal	section	# of sections	file number	Image J area		% of bone per section	Total % per animal
				total area	defect area		
1	a	1	P9070001	136829		0.61	0.35
		2	P9070001		829		
	b	1	P9070001	193264		0.00	
					0		
2	only one	1	e2w-2 only section	96141		3.88	3.88
		2	e2w-2 only section		1039		
		3	e2w-2 only section		1783		
		4	e2w-2 only section		280		
		5	e2w-2 only section		229		
		6	e2w-2 only section		398		
					3729		
3	a	1	e2w-3a	185129		0.32	0.67
		2	e2w-3a		358		
		3	e2w-3a		120		
		4	e2w-3a		113		
					591		
	b	1	e2w-3b	68813		1.01	
		2	e2w-3b		438		
		3	e2w-3b		256		
					694		

Animal	section	# of sections	file number	Image J area		% of bone per section	Total % per animal
				total area	defect area		
4	a	1	e2w-4a	68308		21.50	10.8
		2	e2w-4a		7862		
		3	e2w-4a		2100		
		4	e2w-4a		1195		
		5	e2w-4a		1829		
		6	e2w-4a		1703		
					14689		
	b	1	e2w-4b	100864		0.10	
		2	e2w-4b		185		
		3	e2w-4b		93		
		4	e2w-4b		608		
		5	e2w-4b		122		
					1008		
5	a	1	e2w-5a	41820		4.65	3.77
		2	e2w-5a		690		
		3	e2w-5a		274		
		4	e2w-5a		979		
					1943		
	b	1	e2w-5b	71501		2.89	
		2	e2w-5b		794		
		3	e2w-5b		524		
		4	e2w-5b		214		
		5	e2w-5b		533		
					2065		
6	a	1	e2w-6a	152437		30.31	25.46
		2	e2w-6a		658		
		3	e2w-6a		5628		
		4	e2w-6a		1304		
		5	e2w-6a		28872		
		6	e2w-6a		8761		
		7	e2w-6a		978		
					46201		
	b	1	e2w-6b	159752		20.61	
		2	e2w-6b		227		
		3	e2w-6b		18617		
		4	e2w-6b		1205		
		5	e2w-6b		10069		
		6	e2w-6b		2807		
					32925		

8	a	1	e2w-8a	207192		27.96	26.94
		2	e2w-8a		32269		
		3	e2w-8a		20732		
		4	e2w-8a		4925		
					57926		
	b	1	e2w-8b	177039		25.92	
		2	e2w-8b		13743		
		3	e2w-8b		13869		
		4	e2w-8b		18278		
					45890		

Table A.2 Area in the defect occupied by new bone calculated both in absolute values by "Image J" software and as percentages of the entire defect area at 2 weeks.

4 week group analysis

TREATMENT GROUP	SPECIMEN/ SLIDE NUMBER
Control (DuraGen & saline)	1, 2
Ematrix™ (DuraGen & Ematrix™)	3, 4, 5
rhBMP-2 (DuraGen & rhBMP-2)	6, 7, 8

Table A.3 Distribution of animals (their identifying number) into the experimental groups at 4 weeks.

Animal	Sections & file number			Image J area		% of bone in section	Total % of bone in defect
				new bone	total defect		
1	A	1	e4w-1a		70813	23.83	20.03
		2	e4w-1a	885			
		3	e4w-1a	123			
		4	e4w-1a	87			
		5	e4w-1a	61			
		6	e4w-1a	178			
		7	e4w-1a	357			
		8	e4w-1a	2776			
		9	e4w-1a	2108			
		10	e4w-1a	2414			
		11	e4w-1a	1852			
		12	e4w-1a	3624			
		13	e4w-1a	1683			
		14	e4w-1a	730			
				16878			
	B	1	e4w-1b		31953	16.22	
		2	e4w-1b	213			
		3	e4w-1b	122			
		4	e4w-1b	70			
		5	e4w-1b	1258			
		6	e4w-1b	652			
	only	7	e4w-1b	2867			
2	section	1	e4w-2	**5182**	64679	0.00	0
				0			
	only		e4w-3-only				
3	sect	1	section		35862	36.23	36.23
			e4w-3-only				
		2	section	**12993**			

4	A	1	e4w-4a		82264	22.55	21.70
		2	e4w-4a	13750			
		3	e4w-4a	988			
		4	e4w-4a	786			
		5	e4w-4a	263			
		6	e4w-4a	442			
		7	e4w-4a	2318			
				18547			
	B	1	e4w-4b		71784	20.84	
		2	e4w-4b	2889			
		3	e4w-4b	144			
		4	e4w-4b	3977			
		5	e4w-4b	7950			
				14960			

5	A	1	e4w-5a		63722	77.62	62.70
		2	e4w-5a	22672			
		3	e4w-5a	1360			
		4	e4w-5a	12660			
		5	e4w-5a	10931			
		6	e4w-5a	1835			
				49458			
	B	1	e4w-5b		69223	47.78	
		2	e4w-5b	5135			
		3	e4w-5b	386			
		4	e4w-5b	5296			
		5	e4w-5b	15885			
		6	e4w-5b	6373			
				33075			

6	A	1	e4w-6a		44848	34.82	54.89
		2	e4w-6a	8274			
		3	e4w-6a	1108			
		4	e4w-6a	713			
		5	e4w-6a	1741			
		6	e4w-6a	3780			
				15616			
	B	1	e4w-6b		40112	74.96	
		2	e4w-6b	9014			
		3	e4w-6b	3496			
		4	e4w-6b	2420			
		5	e4w-6b	239			
		6	e4w-6b	14898			
				30067			

7	a	1	e4w-7a		96828	41.21	45.28
		2	e4w-7a	27678			
		3	e4w-7a	798			
		4	e4w-7a	12565			
		5	e4w-7a	3707			
				44748			
	b	1	e4w-7b		50449	49.35	
		2	e4w-7b	769			
		3	e4w-7b	3898			
		4	e4w-7b	318			
		5	e4w-7b	982			
		6	e4w-7b	4123			
		7	e4w-7b	8691			
		8	e4w-7b	6117			
				24898			
8	a	1	e4w-8 only section		48181	27.67	27.67
		2	e4w-8 only section	1025			
		3	e4w-8 only section	815			
		4	e4w-8 only section	7518			
		5	e4w-8 only section	623			
		6	e4w-8 only section	3353			
				13334			

Table A.4 Area in the defect occupied by new bone calculated both in absolute values by "Image J" software and as percentages of the entire defect area at 4 weeks.

6 week group analysis

TREATMENT GROUP	SPECIMEN/ SLIDE NUMBER
Control (DuraGen & saline)	1, 6
Ematrix™ (DuraGen & Ematrix™)	3, 4, 5
rhBMP-2 (DuraGen & rhBMP-2)	7, 8, 9

Table A.5 Distribution of animals (their identifying number) into the experimental groups at 6 weeks.

	Sections		Image J area new bone	Image J area total defect	Sections		Image J area new bone	Image J area total defect
Animal 1		E6w-1a		173336		E6w-1b		131876
	2	E6w-1a	238		2	E6w-1b	175	
	3	E6w-1a	689		3	E6w-1b	108	
	4	E6w-1a	23459		4	E6w-1b	57	
	5	E6w-1a	373		5	E6w-1b	487	
	6	E6w-1a	162				**827**	
	7	E6w-1a	189					
			25110					
	% of bone		14.49				0.63	7.56
Animal 3		E6w-3a		281035		E6w-3b		225474
	2	E6w-3a	201		2	E6w-3b	211	
	3	E6w-3a	11892		3	E6w-3b	278	
	4	E6w-3a	1013		4	E6w-3b	4021	
	5	E6w-3a	1047		5	E6w-3b	336	
	6	E6w-3a	52149		6	E6w-3b	85	
	7	E6w-3a	2122		7	E6w-3b	1173	
	8	E6w-3a	320		8	E6w-3b	4243	
	9	E6w-3a	11016		9	E6w-3b	808	
			79760		10	E6w-3b	1086	
							12241	
	% of bone		28.38				5.43	16.905

Animal 4								
		E6w-4a		325345		E6w-4b		259758
	2	E6w-4a	1665		2	E6w-4b	11346	
	3	E6w-4a	423		3	E6w-4b	3958	
	4	E6w-4a	44908		4	E6w-4b	426	
	5	E6w-4a	27586		5	E6w-4b	2759	
	6	E6w-4a	39896		6	E6w-4b	266	
	7	E6w-4a	35229		7	E6w-4b	139	
	8	E6w-4a	408		8	E6w-4b	7854	
			21445		9	E6w-4b	263	
					10	E6w-4b	39194	
					11	E6w-4b	19432	
							85637	
	% of bone		6.59				32.97	19.78

Animal 5								
		E6w-5a		216494		E6w-5b		162448
	2	E6w-5a	65804		2	E6w-5b	455	
	3	E6w-5a	3999		3	E6w-5b	1669	
	4	E6w-5a	4882		4	E6w-5b	500	
	5	E6w-5a	912		5	E6w-5b	812	
	6	E6w-5a	41177		6	E6w-5b	291	
			116774		7	E6w-5b	5045	
							8772	
	% of bone		53.94				5.4	29.67

Animal 6								
		E6w-6a		187484		E6w-6b		155278
	2	E6w-6a	1416		2	E6w-6b	373	
	3	E6w-6a	968		3	E6w-6b	219	
	4	E6w-6a	139		4	E6w-6b	12124	
	5	E6w-6a	2037		5	E6w-6b	708	
			4560		6	E6w-6b	2970	
					7	E6w-6b	1262	
					8	E6w-6b	8172	
							25828	
	% of bone		2.43				16.63	9.53

Animal 7		E6w-7a		196829		E6w-7b		171421
	2	E6w-7a	701		2	E6w-7b	150	
	3	E6w-7a	15026		3	E6w-7b	8239	
	4	E6w-7a	10220		4	E6w-7b	6906	
			25947		5	E6w-7b	289	
					6	E6w-7b	468	
					7	E6w-7b	5636	
							21688	
	% of bone		13.18				12.65	12.915

Animal 8		E6w-8a1		226949		E6w-8b2		196007
	2	E6w-8a1	11778		2	E6w-8b2	49785	
	3	E6w-8a1	434		3	E6w-8b2	3463	
	4	E6w-8a1	439		4	E6w-8b2	3580	
	5	E6w-8a1	1901		5	E6w-8b2	1029	
	6	E6w-8a1	1002		6	E6w-8b2	3082	
	7	E6w-8a1	401		7	E6w-8b2	723	
	8	E6w-8a1	35035		8	E6w-8b2	535	
	9	E6w-8a1	559		9	E6w-8b2	1433	
	10	E6w-8a1	175		10	E6w-8b2	10378	
	11	E6w-8a1	2782		11	E6w-8b2	616	
	12	E6w-8a1	592		12	E6w-8b2	9324	
	13	E6w-8a1	2394				**83948**	
	14	E6w-8a1	22775					
			80267					
	% of bone		35.37				42.83	39.1

Animal 9		E6w-9a1		186788		E6w-9b2		199463
	2	E6w-9a1	26387		2	E6w-9b2	1307	
	3	E6w-9a1	6094		3	E6w-9b2	10123	
			32481		4	E6w-9b2	598	
					5	E6w-9b2	1276	
					6	E6w-9b2	71	
					7	E6w-9b2	1024	
					8	E6w-9b2	69	
					9	E6w-9b2	93	
					10	E6w-9b2	288	
					11	E6w-9b2	2527	
					12	E6w-9b2	274	
					13	E6w-9b2	3648	
					14	E6w-9b2	305	
					15	E6w-9b2	138	
					16	E6w-9b2	553	
					17	E6w-9b2	173	
							22467	
	% of bone		17.39				11.26	14.325

Table A.6 Area in the defect occupied by new bone calculated both in absolute values by "Image J" software and as percentages of the entire defect area at 6 weeks.

REFERENCES

Albrektsson T, Johansson C. Osteoinduction, osteoconduction and osseointegration. *Eur Spine J.* 2001;10:S96-S101.

Alsberg E, Hill EE, Mooney DJ. Craniofacial tissue engineering. *Crit Rev Oral Biol Med*. 2001;12:64-75.

Anderson JM. Biocompatibility of Tissue Engineered Implants, 1998, in *Frontiers in Tissue Engineering,* McIntyre LV, Ed., Pergamon. p.156, 165.

Blom EJ, Klein-Nulend J, Yin L, van Waas MAJ, Burger EH. Transforming growth factor-β1 incorporated in calcium phosphate cement stimulates osteotransducivity in rat calvarial bone defects. *Clin Oral Impl Res.* 12(6):609-616, 2001.

Bosch VC, Dalstra M, Wikesjö UME, Trombelli L. Healing patterns in calvarial bone defects following guided bone regeneration in rats. A micro-CT scan analysis. *J Clin Periodontol.* 2002;29:865-870.

Bosnakovski D, Mizuno M, Kim G, Takagi S, Okumura M, Fujinaga T. Chondrogenic differentiation of bovine bone marrow mesenchymal stem cells (MCSs) in different hydrogels: influence of collagen type II extracellular matrix in MSC chondrogenesis. *Biotechnol Bioeng.* 2006;93:1052-1063.

Burdick JA, Anseth KS. Photoencapsulation of osteoblasts in injectable RGD-modified PEG hydrogels for bone tissue engineering. *Biomaterials.* 2002;23:4315-4323.

Chen F, Mao T, Tao K, Chen S, Ding G, Gu X. Injectable bone. *Bt J Oral Maxillofac Surg.* 200341:240-243.

Danish SF, Samdani A, Hanna A, Storm P, Sutton L. Experience with acellular human dura and bovine collagen matrix for duroplasty after posterior fossa decompression for Chiari malformations. *J Neurosurg.* 2006;104(1 Suppl):16-20.

Davies JE (ed). Bone Engineering. © 2000 em squared incorporated. Chapters 40, 42, 45, 46 and 52.

Donos N, Lang NP, Karoussis IK, Bosshardt D, Tonetti M, Kostopoulos L. Effect of GBR in combination with deproteinized bovine bone mineral and/ or enamel matrix proteins on the healing of critical-size defects. *Clin Oral Impl Res.* 2004;15:101-111.

Earthman JC, Sheets CG, Paquette JM, Kaminishi RM, Nordland WP, Keim RG, Wu JC. Tissue engineering in dentistry. *Clin Plast Surg*. 2003;30:621-639.

Elisseeff J, Puleo C, Yang F, Sharma B. Advances in skeletal tissue engineering with

hydrogels. *Orthod Craniofacial Res.* 2005;8:150-161.

Ferreira GR, Cestari TM, Granjeiro JM, Taga R. Lack of repair of rat skull critical size defect treated with bovine morphometric protein bound to microgranular bioabsorbable hydroxyapatite. *Braz Dent J.* 200415:175-180.

Frost HM. The biology of fracture healing. An overview for clinicians, part I. *Clin Orthop Rel Res.* 1989;248:283-293.

Gysin R, Wergedal JE, Sheng MH-C, Kasukawa Y, Miyakoshi N, Chen S-T, Peng H, Lau K-HW, Mohan S, Baylik DJ. Ex vivo gene therapy with stromal cells transduced with a retroviral vector containing the BMP4 gene completely heals critical size calvarial defect in rats. *Gene Therapy*. 2002;9:991-999.

Handschel J, Wiesmann HP, Stratmann U, Kleinheinz J, Meyer U, Joos U. TCP is hardly resorbed and osteoconductive in a non-loading calvarial model. *Biomaterials.* 2002;23:1689-1695.

Hollinger JO, Einhorn TA, Doll BA, Sfeir C (ed). Bone Tissue Engineering. © 2005 by CRC Press. Chapters 5, 6 and 9.

Hollinger JO, Kleimschmidt JC. The critical size defect as an experimental model to test bone repair materials. *J Craniofac Surg.* 1990;1:60-68.

Hu Y, Hollinger JO, Marra KG. Controlled release from coated polymer microparticles embedded in tissue-engineered scaffolds. *J Drug Targeting.* 2001;9:431-438.

Karagiri T, Yamaguchi A, Ikeda T, Yoshiki S, Wozney V, Rosen V, Wang EA, Tanaka H, Omura S, Suda T. The non-osteogenic mouse pluripotent cell line, C3H10T1/2, is induced to differentiate into osteoblastic cells by recombinant human bone morphogenetic protein-2. *Biochem Biophys Res Commun.* 1990;172:295-299.

Kenley R, Marden L, Turek T, Jin L, Ron E, Hollinger JO. Osseous regeneration in the rat calvarium using novel delivery systems for recombinant human bone morphogenetic protein-2 (rhBMP-2). *J Biomed Mater Res.* 1994;28:1139-1147.

Langer R, Vacanti JP. Tissue engineering Science. 1993;260:920-926. Review

Lim SC, Lee ML, Yeo HH. Effects of various materials on regeneration of calvarial defects in rats. *Pathol Int.* 2000;50:594-602.

Lind M. Growth factors: possible new clinical tools. *Acta Orthop Scand.* 1996;67:407-417.

Linde A, Hedner E. Recombinant bone morphogenetic protein-2 enhances bone healing, guided by osteopromotive e-PTFE membranes: an experimental study in rats. *Calcif*

Tissue Int. 1995;56:549-553.

Lutolf MP, Weber FE, Schmoekel HG, Schense JC, Kohler T, Müller R and Hubbell JA Repair of bone defects using synthetic mimetics of collagenous extracellular matrices. *Nat Biotechnol.* 2003;21:513-518.

Marden LJ, Hollinger JO, Chaudhari A, Turek T, Schaub RG, Ron E. Recombinant human bone morphogenetic protein-2 is superior to demineralized bone matrix in repairing craniotomy defects in rats. *J Biomed Mater Res.* 1994;28:1127-1138.

Moon HJ, Kim KN, Kim KM, Choi SH, Kim CK, Kim KD, LeGeros RZ, Lee YK. Bone formation in calvarial defects of Sprague-Dawley rats by transplantation of calcium phosphate glass. *J Biomed Mater Res A.* 2005;74:497-502.

Narotam PK, José S, Nathoo N, Taylon C, Vora Y. Collagen matrix (Duragen®) in Dural repair: analysis of a new modified technique. *Spine.* 2004;29:2861-2867.

Nguyen H, Qian JJ, Bhatnagar RS, Li S. Enhanced cell attachment and osteoblastic activity by P-15 peptide-coated matrix in hydrogels. *Biochem Biophys Res Commun.* 2003;311:179-186.

Pang EK, Im SU, Kim CS, Choi SH, Chai JK, Kim CK, Han SB, Cho KS. Effect of recombinant human bone morphogenetic protein-4 dose on bone formation in a rat calvarial defect model. *J Periodontol.* 2004;75:1364-1370.

Passos-Bueno MR, Wilcox WR, Jabs EW, Sertel AL, Alonso LG, Kitoh H. Clinical spectrum of fibroblast growth factor receptor mutations. *Hum Mutat.* 1999;14:115-125.

Payne RG, McGonigle JS, Yaszemski MJ, Yasko AW, Mikos AG. Development of an injectable, in situ crosslinkable, degradable polymeric carrier for osteogenic cell populations. Part 3. Proliferation and differentiation of encapsulated marrow stromal osteoblasts cultured on crosslinking poly(propylene fumarate). *Biomaterials.* 2002;23:4381-4387.

Pollok JM, Vacanti JP. Tissue engineering. *Semin Pediatr Surg*. 1996;5:191-196.

Pryor ME, Yang J, Polimeni G, Koo KT, Hartman MJ, Gross H, Agelan A, Manns JM, Wikesjö UME. Analysis of rat calvaria defects implanted with a platelet-rich plasma preparation: radiographic observations. *J Periodontol.* 2005;76:1287-1292.

Rabinowitz L, Monnerie H, Shashidhara S, Le Roux PD. Growth of rat cortical neurons in Duragen®, a collagen-based dual graft matrix. *Neurol Res.* 2005;27:887-894.

Reddi AH. Morphogenesis and tissue engineering of bone and cartilage: inductive signals,

stem cells and biomimetic materials. *Tissue Eng*. 2000;6:351-359.

Reddi AH. Role of morphogenetic proteins in skeletal tissue engineering and regeneration. *Nat Biotechnol*. 1998;16:247-252.

Richardson TR, Peters MC, Ennett AB, Mooney DJ. Polymeric system for dual growth factor delivery, *Nat Biotechnol.* 2001;19:1029-1034.

Rowley JA, Madlambayan G, Mooney DJ. Alginate hydrogels as synthetic extracellular matrix materials. *Biomaterials.* 1999;20:45-53.

Ruppert R, Hoffmann E, Sebald W. Human bone morphogenetic protein 2 contains heparin-binding site which modifies its biological activity. *Eur J Biochem.* 1996;237:295-302.

Senn N. On the healing of aseptic bone cavities by implantation of antiseptic decalcified bone. *Am J Med Sci.* 1889;98:219-243.

Schmitz JP, Hollinger JO. The critical size defect as an experimental model for cranio-mandibulo-facial non-unions. *Clin Orthop Relat Res.* 1986;205:299-308.

Schmoekel H, Schense JC, Weber FE, Grätz KW, Gnägi D, Müller R, Hubbell JA. Bone healing in the rat and dog with nonglycosylated BMP-2 demonstrating low solubility in fibrin matrices. *J Orthop Res.* 2004;22:376-381.

Schmoekel HG, Weber FE, Schense JC, Grätz KW, Schawalder P, Hubbell JA. Bone repair with a form of BMP-2 engineered for incorporation into fibrin cell ingrowth matrices. *Biotechnol Bioeng.* 2005;89:253-262.

Sieron AL, Louneva N, Fertala A. Site-specific interaction of bone morphogenetic protein 2 with procollagen II. *Cytokine.* 2002;18:214-221.

Sikavitsas VI, Van den Dolder J, Bancroft GN, Jansen JA, Mikos AG. Influence of the in vitro culture period on the in vivo performance of cell/titanium bone tissue-engineered constructs using a rat cranial critical size defect model. *J Biomed Mater Res.* 2003;67:944-951.

Sirola K. Regeneration of defects in the calvaria: an experimental study. *Ann Med Exp Biol Finland.* 1960;38(Suppl 2):1-87.

Smentana K. Cell biology of hydrogels. *Biomaterials.* 1993;14:1046-1050.

Sweeney TM, Opperman LA, Persing MD, Ogle RC, Repair of critical size rat calvarial defects using extracellular matrix protein gels. *J Neurosurg*. 1995;83:710-715.

Temenoff JS, Mikos AG. Injectable biodegradable materials for orthopedic tissue

engineering. *Biomaterials.* 2000;21:2405-2012.

Thaller SR, Dart A, Tesluk H. The effects of insulin-like growth factor on critical-size calvarial defects in Sprague-Dawley rats. *Ann Plast Surg.* 1993;31:429-433.

Thies RS, Bauduy M, Ashton A, Kurtzberg L, Wozney JM, Rosen V. Recombinant human bone morphogenetic protein-2 induces osteoblastic differentiation in W-20-17 stromal cells. *Endocrinology.* 1992;172:295-299.

Trojani C, Boukhechba F, Scimeca JC, Vandenbos F, Michiels JF, Daculsi G, Boileau P, Weiss P, Carle GF, Rochet N. Ectopic bone formation using an injectable biphasic calcium phosphate/ Si-HPMC hydrogel composite loaded with undifferentiated bone marrow stromal cells. *Biomaterials.* 2006;27:3256-3264.

Wang EA, Rosen V, D'Alessandro JS, Bauduy M, Cordes P, Harada T, Israel DI, Hewick RM, Kerns KM, LaPan P, Luxemberg DP, McQuaid D, Moutsatsos IK, Nove J, Wozney JM. Recombinant human bone morphogenetic protein induces bone formation. *Proc Natl Acad Sci USA.* 1990;87:2220-2224.

Wilson-Hench J. Osteoconduction (1987). In: Williams DF (ed). Progress in biomedical engineering, vol.4 Definitions in biomaterials. Elsevier, Amsterdam, p.29.

Woo BH, Fink BF, Page R, Schrier JA, Jo YW, Jiang G, DeLuca M, Vasconez HC, DeLuca PP. Enhancement of bone growth by sustained delivery of recombinant human bone morphogenetic protein-2 in a polymeric matrix. *Pharm Res.* 2001;18:1747-1753.